NASA TN D-1012

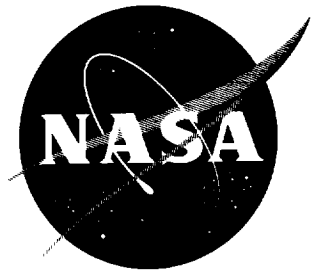

TECHNICAL NOTE

D-1012

EQUATIONS OF MOTION AND DESIGN CRITERIA FOR THE DESPIN OF A VEHICLE BY THE RADIAL RELEASE OF WEIGHTS AND CABLES OF FINITE MASS

By Donald G. Eide and Chester A. Vaughan

Langley Research Center
Langley Air Force Base, Va.

NATIONAL AERONAUTICS AND SPACE ADMINISTRATION
WASHINGTON January 1962

NATIONAL AERONAUTICS AND SPACE ADMINISTRATION

TECHNICAL NOTE D-1012

EQUATIONS OF MOTION AND DESIGN CRITERIA FOR THE DESPIN OF A VEHICLE BY THE RADIAL RELEASE OF WEIGHTS AND CABLES OF FINITE MASS

By Donald G. Eide and Chester A. Vaughan

SUMMARY

The equations of motion are derived for the despinning of a rigid-body payload by the use of weights attached to the ends of unwinding cables of finite mass that are released when colinear with a radius of the payload. Expressions for the length of cable of a given mass per unit length or mass of attached weights required to despin a body to zero rotational speed are derived. The energy and momentum balance equations of initial and final conditions are presented which must be solved simultaneously for either the length of cable or mass required to despin a payload to a spin rate other than zero. The effect of cable mass is significant on the desired spin-reduction ratio. The effects on the residual spin due to an error in body moment of inertia, cable length, and release of cables and weights at an angle other than the desired 90° are shown. The expected errors in inertia produce the largest errors in residual spin.

The maximum payload deceleration and maximum cable tension are presented for various nondimensional parameters. The effect of the spin-reduction ratio on the peak deceleration is discussed. Reduction in the maximum payload deceleration and cable tension may be obtained by proper staging of the despin, lowering the initial spin rate, and using lighter weights. An expression for the total time required to despin is presented and found to be within 0.5 percent of the actual time required.

INTRODUCTION

The use of spin stabilization on the last stages of launch vehicles to maintain orbit injection angles to within specific tolerances has proven very reliable. However, as satellite and probe experiments become more complex, payloads with a required spin rate much lower than that required for stabilization at injection or a nonspinning platform is

required. In order to be able to utilize spin stabilization for the initial injection and still have reduced spin rate or a nonspinning platform for the actual experiment, retrojets or unwinding small weights on the end of flexible cables may be used.

Retrojets require an accurate knowledge of the initial spin rate and the moment of inertia about the spin axis for achieving either a fractional reduction in spin or complete despin. Unwinding weights, first proposed by the Jet Propulsion Laboratory of California Institute of Technology, also require an accurate knowledge of the initial spin rate for a fractional reduction in rotational velocity and an accurate knowledge of the moment of inertia about the spin axis. This so-called "yo-yo" system is completely independent of initial spin rate when a reduction to zero spin is required, and thereby greatly adds to the simplicity of the system. The accuracy in achieving zero spin is dependent on the accuracy of the physical constants involved, such as the moment of inertia, length and mass of the cable, mass of the attached weights, and the ability to release the weights at the proper time. This type of system, which has been used on a number of satellites, has been mentioned in reference 1 and studied in reference 2 where the weight of the cable is considered negligible and in reference 3 where the weight of cable is included by means of an approximation.

This report derives the equations for: (1) initial and final energy and angular momentum which are used to determine the cable length or mass of weights required for zero spin and despin to any desired ratios of final to initial spin rates, (2) residual spin as a function of the physical quantities from which an error analysis may be made, and (3) the transient conditions from the initial start of the unwinding cables of significant weight to the release of the cables and weights when they are extending radially from the center of the payload. The transient conditions are checked experimentally by taking high-speed motion pictures of a despin to zero rotational speed of an initially rotating cylinder.

Results are presented for the following:

(1) Ratios of payload inertia to initial mass inertia of 50, 100, 200, 300, and 400

(2) Ratios of final to initial spin rates of 0.0, 0.05, 0.1, and 0.2

(3) Ratios of cable weight to attached weights of 0.0, 0.5, 1.0, and 1.5

(4) Maximum payload deceleration

(5) Maximum cable tension

(6) Effect of cable release at an angle to the desired radial position.

The effects on the desired spin by percent errors up to 10 percent of the inertia and for 0.25 percent of the cable length are shown. An equation for the determination of the total time to despin any configuration to any residual spin rate is presented.

SYMBOLS

E	total energy of rotating system, ft-lb
F	cable tension, lb
H	angular momentum, ft-lb-sec
I	moment of inertia of body about roll axis, slug-ft^2
K	total mass of cables per foot, $\sum_{i=1}^{n} K_i$, slugs/ft
L	length of flexible cable from surface of payload to center of mass of weights, ft
l	distance along cable to a differential element of cable mass
M	total mass of weights, $\sum_{i=1}^{n} M_i$, slugs
m_i	mass of ith cable, $K_i L$, slugs
n	number of weights and number of cables, equal to or greater than 2
R	radius of body about roll axis, ft
T	kinetic energy, ft-lb
t	total time to despin, sec
V	linear velocity, ft/sec
X,Y	fixed coordinate system

x,y	rotating coordinate system in phase II
α	angle in phase II from x-axis to extended cables, radians
θ	angle subtended by X-axis of fixed coordinate system and line fixed to rotating payload from center of rotation, radians
λ	spin-reduction ratio, that is, ratio of final spin rate to initial spin rate, $\dot{\theta}_f/\dot{\theta}_o$
$\Delta\lambda$	error in residual spin, $\lambda_a - \lambda_d$
ϕ	angle subtended by line fixed to rotating payload from center of rotation and line from center of payload to point of cable contact with payload circumference, radians
ψ	angle subtended by line from center of payload to point of cable contact with payload circumference and line from center of payload to original point of contact of jth particle on payload circumference, radians

Subscripts:

a	actual
C	pertaining to cables
d	desired
f	final conditions
i	ith cable or weight
j	jth particle in ith cable
M	pertaining to weights
max	maximum
o	initial conditions
P	pertaining to payload

Dots over symbols represent derivatives with respect to time.

THEORY

To obtain a fractional reduction or a complete removal of rotational speed from a spinning body by the use of weights and flexible cables involves the transfer of the initial angular momentum in the payload and packaged despin mechanism to the unwound weight and cable system. At the precise moment that the weight and cable system contains the desired proportion of the initial angular momentum, they are released from the body leaving it with the desired momentum and hence the desired spin. In order to analyze the despin system, the following assumptions are made:

(1) System is conservative.

(2) Effect of gravity is neglected.

(3) Weights are considered point masses.

(4) Cables are flexible, unstretchable, and of uniform mass per unit length.

(5) Motion is two-dimensional.

(6) Unwound portion of the cable is a straight line.

Fixed reference axes are chosen with the origin coinciding with the center of the rotating body, as seen in figure 1. Therefore, the only energies to be considered are those of the body and weights rotating about the origin and those of the cables rotating about the origin and their own centers of mass. The weights and cables are paired so that the motion is symmetric about the origin. Therefore, the center of mass of the system is at the origin of the fixed coordinate system.

The final position of the weights and cables for release is chosen at the moment they are colinear with a radius from the center of the rotating body (payload). (See fig. 1.) This position is chosen to reduce the error in residual spin induced by a possible release of the weights at an angle other than $\alpha = 90^{\circ}$.

Derivation of Equations To Determine Length of Cable or Mass Required To Obtain Zero Residual Spin

In order to find the length of cable required to obtain zero residual spin in the payload, the initial and final angular momentum and kinetic energy are equated.

For the angular momentum balance

$$H_o = \sum_{i=1}^{n} H_{Mi,f} + \sum_{i=1}^{n} H_{Ci,f} \tag{1}$$

where

$$H_o = \left(I + \sum_{i=1}^{n} M_i R^2 + \sum_{i=1}^{n} K_i L R^2\right)\dot{\theta}_{P,o} \tag{2}$$

$$\sum_{i=1}^{n} H_{Mi,f} = \sum_{i=1}^{n} M_i (L + R)^2 \dot{\theta}_{Mi,f} \tag{3}$$

When $\dot{\theta}_{P,f} = 0$,

$$\dot{\theta}_{Mi,f} = \frac{L\dot{\alpha}_{Mi,f}}{L + R} \tag{4}$$

To find the angular momentum of the cables, reference is made to figure 1. The angular momentum of the jth particle on the ith cable at the instant of release is

$$dH_{Ci,f} = (l + R)^2 \dot{\theta}_{Ci,f} dm_i$$

where $l + R$ is the distance of the jth particle from the origin.

The rotation of the jth particle about the origin at the final instant can be stated as

$$\dot{\theta}_{Cj,f} = \frac{l\dot{\alpha}_{Ci,f}}{l + R}$$

and the incremental mass as

$$dm_i = K_i \, dl$$

Therefore,

$$dH_{Ci,f} = K_i (l + R)^2 \frac{l\dot{\alpha}_{Ci,f}}{l + R} \, dl$$

$$H_{Ci,f} = K_i \dot{\alpha}_{Ci,f} \int_0^L (l + R) l \, dl$$

and

$$H_{C,f} = \sum_{i=1}^{n} H_{Ci,f} = \left[\sum_{i=1}^{n} \left(\frac{K_i L^3}{3} + \frac{K_i R L^2}{2} \right) \right] \dot{\alpha}_{Ci,f} \tag{5}$$

Equation (5) gives the angular momentum of the cable about the origin which includes the angular momentum of the cable about its own center of mass.

With the assumption that the individual weights are of equal mass and that the individual cables are of equal length and mass per unit length,

$$\sum_{i=1}^{n} M_i = M$$

$$\sum_{i=1}^{n} K_i = K$$

With these relationships and by substituting equations (2) to (5) into equation (1), the following equation results:

$$\left(I + MR^2 + KLR^2 \right) \dot{\theta}_{P,o} = \left[M(L + R)L + \frac{KL^3}{3} + \frac{KRL^2}{2} \right] \dot{\alpha}_f \tag{6}$$

where

$$\dot{\alpha}_f = \dot{\alpha}_{C,f} = \dot{\alpha}_{M,f}$$

The energy balance of the system is

$$T_o = \sum_{i=1}^{n} T_{Mi,f} + \sum_{i=1}^{n} T_{Ci,f} \tag{7}$$

where

$$T_o = \frac{1}{2}\left(I + \sum_{i=1}^{n} M_i R^2 + \sum_{i=1}^{n} K_i L R^2\right)\dot{\theta}_{P,o}{}^2 \tag{8}$$

and

$$T_{M,f} = \sum_{i=1}^{n} T_{Mi,f} = \frac{1}{2}\sum_{i=1}^{n} M_i (L + R)^2 \dot{\theta}_{Mi,f}{}^2$$

or substituting the value previously obtained for $\dot{\theta}_{Mi,f}$ in equation (4) and summing, from i = 1 to n, leads to

$$T_{M,f} = \frac{ML^2 \dot{\alpha}_f{}^2}{2} \tag{9}$$

To find the energy of the cables, refer again to figure 1. The incremental energy is

$$dT_{Ci,f} = \frac{1}{2}(l + R)^2 \dot{\theta}_{Ci,f}{}^2 dm_i$$

Substituting previously determined values for these quantities results in

$$\sum_{i=1}^{n} dT_{Ci,f} = \frac{1}{2}\sum_{i=1}^{n} (l + R)^2 \frac{l^2 \dot{\alpha}_{Ci,f}{}^2 K_i}{(l + R)^2}\, dl$$

Integrating and summing the parts gives

$$T_{C,f} = \frac{KL^3}{6}\dot{\alpha}_f{}^2 \tag{10}$$

This represents the sum of the kinetic energies of the cables moving about the origin and the sum of the kinetic energies of the cables about their own center of mass. Therefore, substituting equations (8), (9), and (10) into equation (7) yields

$$\left(\frac{I + MR^2 + KLR^2}{2}\right)\dot{\theta}_{P,o}{}^2 = \left(\frac{ML^2}{2} + \frac{KL^3}{6}\right)\dot{\alpha}_f{}^2 \tag{11}$$

Solving equations (6) and (11) for $\frac{\dot{\theta}_{P,o}^2}{\dot{\alpha}_f^2}$ and equating the results yields

$$M + \frac{KL}{3} = \frac{\left[\frac{KL^2}{3} + \left(\frac{KR}{2} + M\right)L + MR\right]^2}{I + MR^2 + KLR^2}$$

or, in terms of L as a quartic equation,

$$\frac{K^2}{9}L^4 + \left(\frac{K^2R}{3} + \frac{2}{3}KM\right)L^3 + \left(M^2 + \frac{5}{3}KMR - \frac{K^2R^2}{12}\right)L^2$$

$$+ \left(2M^2R - \frac{KMR^2}{3} - \frac{IK}{3}\right)L - IM = 0 \qquad (12)$$

Equation (12) is then solved for L. The solution for L will yield either one pair of complex roots (one negative real root and one positive real root) or three negative roots and one positive root. From the physical situation the positive real root is the length required to achieve zero residual spin. An alternate method would be to choose a length of cable and solve equation (12) for the mass of the weights, since only M and M^2 terms are involved.

For the case where the cable mass is considered negligible, the solution for L reduces to

$$L = R\left(\sqrt{\frac{I}{MR^2} + 1} - 1\right) \qquad (13)$$

Derivation of Equations To Determine the Length of Cable or Mass of Weights Required To Obtain Any Desired Residual Spin Rate

In order to find the length of cable or mass of the weight required to obtain a desired residual spin, the same procedure is adopted for the angular momentum and energy balance. In this case the initial rotational speed must be known to whatever end accuracy is desired.

For the angular momentum

$$H_o = H_{M,f} + H_{C,f} + H_{P,f} \tag{14}$$

where

$$H_o = (I + MR^2 + KLR^2)\dot{\theta}_{P,o} \tag{15}$$

$$H_{P,f} = I\dot{\theta}_{P,f} \tag{16}$$

and

$$H_{M,f} = M(L + R)^2\dot{\theta}_{M,f}$$

or with

$$\dot{\theta}_{M,f} = \frac{(L + R)\dot{\theta}_{P,f} + L\dot{\alpha}_f}{L + R} \tag{17}$$

the equation for $H_{M,f}$ is

$$H_{M,f} = M(L + R)^2\dot{\theta}_{P,f} + ML(L + R)\dot{\alpha}_f \tag{18}$$

By referring to figure 1, the incremental momentum of the cable can be seen to be

$$dH_{C,f} = K(l + R)^2 \frac{(l + R)\dot{\theta}_{P,f} + l\dot{\alpha}_f}{l + R} dl$$

Therefore,

$$H_{C,f} = \int_0^L \left(K\dot{\theta}_{P,f}l^2 + 2KR\dot{\theta}_{P,f}l + KR^2\dot{\theta}_{P,f} + K\dot{\alpha}_f l^2 + KR\dot{\alpha}_f l\right)dl$$

$$= \left(\frac{KL^3}{3} + KRL^2 + KR^2L\right)\dot{\theta}_{P,f} + \left(\frac{KL^3}{3} + \frac{KRL^2}{2}\right)\dot{\alpha}_f \tag{19}$$

Substituting equations (15), (16), (18), and (19) into equation (14) yields

$$\left(I + MR^2 + KLR^2\right)\dot{\theta}_{P,o} = \left[I + MR^2 + \frac{KL^3}{3} + (M + KR)L^2 + \left(2MR + KR^2\right)L\right]\dot{\theta}_{P,f}$$

$$+ \left[\frac{KL^3}{3} + \left(M + \frac{KR}{2}\right)L^2 + MRL\right]\dot{\alpha}_f \tag{20}$$

For the energy

$$T_o = T_{M,f} + T_{C,f} + T_{P,f} \tag{21}$$

where

$$T_o = \left(\frac{I + MR^2 + KLR^2}{2}\right)\dot{\theta}_{P,o}^{\,2} \tag{22}$$

$$T_{P,f} = \frac{I\dot{\theta}_{P,f}^{\,2}}{2} \tag{23}$$

$$T_{M,f} = \frac{M\left[(L + R)\dot{\theta}_{P,f} + L\dot{\alpha}_f\right]^2}{2} \tag{24}$$

The incremental energy of the cable is

$$dT_{C,f} = \frac{K}{2}\left[(l + R)\dot{\theta}_{P,f} + l\dot{\alpha}_f\right]^2 dl$$

Therefore,

$$T_{C,f} = \frac{K}{2}\int_0^L \left[\left(R^2 + l^2 + 2Rl\right)\dot{\theta}_{P,f}^{\,2} + \left(2l^2 + 2Rl\right)\dot{\theta}_{P,f}\dot{\alpha}_f + l^2\dot{\alpha}_f^{\,2}\right] dl$$

$$= \frac{1}{2}\left[\left(KR^2L + \frac{KL^3}{3} + KRL^2\right)\dot{\theta}_{P,f}^{\,2} + \left(\frac{2KL^3}{3} + KRL^2\right)\dot{\theta}_{P,f}\dot{\alpha}_f + \frac{KL^3}{3}\,\dot{\alpha}_f^{\,2}\right] \tag{25}$$

Substituting equations (22) to (25) into equation (21) yields

$$\left(I + MR^2 + KLR^2\right)\dot{\theta}_{P,o}{}^2 = \left[MR^2 + I + \left(2MR + KR^2\right)L + (KR + M)L^2 + \frac{KL^3}{3}\right]\dot{\theta}_{P,f}{}^2$$

$$+ \left[2MR + (2M + KR)L + \frac{2KL^2}{3}\right]L\dot{\theta}_{P,f}\dot{\alpha}_f + \left(M + \frac{KL}{3}\right)L^2\dot{\alpha}_f{}^2 \qquad (26)$$

Equations (20) and (26) are then solved simultaneously for L or M for any desired ratio of λ, where $\lambda = \frac{\dot{\theta}_{P,f}}{\dot{\theta}_{P,o}}$. In order to simplify this solution, numerical coefficients should be computed to solve these equations.

For the cases considered in this report, the mass of the weights were chosen and then the energy and momentum equations were solved simultaneously for the length of cable by the Newton-Raphson iterative method on the IBM 7090 electronic data processing system.

Solving equations (20) and (26) simultaneously for λ gives

$$\lambda = \frac{A}{B}\left[1 - \sqrt{\frac{C^2(B - A)}{A(BD - C^2)}}\right] \qquad (27)$$

where

$$A = I + MR^2 + KLR^2$$

$$B = I + MR^2 + L^2\left(M + \frac{KL}{3}\right) + 2RL\left(M + \frac{KL}{2}\right) + KR^2L$$

$$C = L^2\left(M + \frac{KL}{3}\right) + RL\left(M + \frac{KL}{2}\right)$$

$$D = L^2\left(M + \frac{KL}{3}\right)$$

Equation (27) may be used to solve for λ if the length of cable and mass of weights are known or assumed. This expression may also be solved to obtain the error introduced in λ for a given error in the moment of inertia and length of cable.

DERIVATION OF THE EQUATIONS OF TRANSIENT MOTION

Lagrange's mechanics are used to obtain the equations of motion for the transient conditions. The motion is considered in two separate phases. In the first phase the cables are completely unwound from the payload until they are extended perpendicular to a radius through the center of rotation of the payload. The second phase starts at the end of phase I with the cables and weights revolving about the point of attachment to the payload. Phase II continues until the cables and weights are colinear with a radius from the center of the payload at which time they are considered released. The equations for the transient motion in both phase I and phase II were programed for and solved on the IBM 7090 electronic data processing system.

L 1 8 3 5

Phase I

During phase I, the X- and Y-axes are fixed in space with their origin coinciding with the center of rotation of the payload. As shown in figure 2, line OB rotates with the payload with an angular velocity of $\dot{\theta}$, and $\dot{\phi}$ is the rate at which the point of tangency (point A) of the cable moves from the original position of the weight at point B. The total energy consists of the rotation of the payload about the origin, and the motion of the weights and cables about the origin:

$$E = \Sigma T = T_P + T_M + T_C \tag{28}$$

where

$$T_P = \left[\frac{I + (KL - KR\phi)R^2}{2}\right]\dot{\theta}^2 \tag{29}$$

$$T_M = \sum_{i=1}^{n} \frac{M_i}{2}\left(\dot{X}_{Mi}^{\,2} + \dot{Y}_{Mi}^{\,2}\right) \tag{30}$$

In order to produce a symmetric problem where the center of mass of the system is located at the origin of the fixed coordinate system, the total number of weights (and hence, the total number of cables used) must be equal to or greater than 2. Therefore,

$$X_{Mi} = R\cos(\theta + \phi) + R\phi\sin(\theta + \phi)$$

$$Y_{Mi} = R\sin(\theta + \phi) - R\phi\cos(\theta + \phi)$$

which yields

$$\dot{X}_{Mi}^2 + \dot{Y}_{Mi}^2 = R^2\phi^2(\dot{\theta} + \dot{\phi})^2 + R^2\dot{\theta}^2 = V_{Mi}^2 \tag{31}$$

Substituting equation (31) into equation (30) yields

$$T_M = \sum_{i=1}^{n} \frac{M_i}{2}\left[R^2\phi^2(\dot{\theta} + \dot{\phi})^2 + R^2\dot{\theta}^2\right] \tag{32}$$

To find the energy of the cables, refer to figure 2; thus

$$dT_{Ci} = \frac{\dot{X}_j^2 + \dot{Y}_j^2}{2}\, dm_i \tag{33}$$

The variable ψ is now introduced which is the angle measured from line OA to line OC. (See fig. 2.) Point C is the point of original contact of the jth particle on the circumference of the payload. The mass of the jth particle on the ith cable is then

$$dm_i = K_i R\, d\psi \tag{34}$$

where $R\, d\psi$ is the incremental length of cable that has unwound. The location of the jth particle on the ith cable relative to the fixed coordinate system is

$$X_j = R\psi \sin(\theta + \phi) + R \cos(\theta + \phi)$$

$$Y_j = -R\psi \cos(\theta + \phi) + R \sin(\theta + \phi)$$

The velocity is then

$$\dot{X}_j = R\psi(\dot{\theta} + \dot{\phi})\cos(\theta + \phi) + R\dot{\psi} \sin(\theta + \phi) - R(\dot{\theta} + \dot{\phi})\sin(\theta + \phi)$$

$$\dot{Y}_j = R\psi(\dot{\theta} + \dot{\phi})\sin(\theta + \phi) - R\dot{\psi} \cos(\theta + \phi) + R(\dot{\theta} + \dot{\phi})\cos(\theta + \phi)$$

However, ψ must increase at the same rate as ϕ; therefore, $\dot{\psi} = \dot{\phi}$ and

$$\dot{X}_j^2 + \dot{Y}_j^2 = R^2\psi^2(\dot{\theta} + \dot{\phi})^2 + R^2\dot{\theta}^2 = V_j^2 \tag{35}$$

Substituting equations (34) and (35) into equation (33) gives

$$dT_{Ci} = \frac{K_i R}{2}\left[R^2\psi^2(\dot{\theta} + \dot{\phi})^2 + R^2\dot{\theta}^2\right]d\psi \tag{36}$$

Therefore, the total kinetic energy of the cables is

$$T_C = \sum_{i=1}^{n} \int_0^{\phi} \frac{K_i R^3}{2}\left[(\dot{\theta} + \dot{\phi})^2\psi^2 + \dot{\theta}^2\right]d\psi$$

Performing the required integration and letting $\sum_{i=1}^{n} K_i = K$ yields

$$T_C = \frac{KR^3\phi}{2}\left[\frac{\phi^2(\dot{\theta} + \dot{\phi})^2}{3} + \dot{\theta}^2\right] \tag{37}$$

Substituting equations (29), (32), and (37) into equation (28) and letting $\sum_{i=1}^{n} M_i = M$ yields

$$T = \left[\frac{I + (KL - KR\phi)R^2}{2}\right]\dot{\theta}^2 + \frac{M}{2}\left[R^2\phi^2(\dot{\theta} + \dot{\phi})^2 + R^2\dot{\theta}^2\right] + \frac{KR^3\phi}{2}\left[\frac{\phi^2(\dot{\theta} + \dot{\phi})^2}{3} + \dot{\theta}^2\right] \tag{38}$$

Now Lagrange's equations are used to determine the equations of motion for the system; since the potential energy is zero, and the system is conservative, Lagrange's equation for θ reduces to

$$\frac{d}{dt}\left(\frac{\partial T}{\partial \dot{\theta}}\right) - \frac{\partial T}{\partial \theta} = 0 \tag{39}$$

Performing the required operations on equation (38) as indicated by equation (39) yields

$$\left[\frac{I}{R^2} + KL + \phi^2\left(M + \frac{KR\phi}{3}\right) + M\right]\ddot{\theta} + \phi^2\left(M + \frac{KR\phi}{3}\right)\ddot{\phi} + \phi\dot{\phi}(\dot{\theta} + \dot{\phi})(2M + KR\phi) = 0 \tag{40}$$

Lagrange's equation for ϕ reduces to

$$\frac{d}{dt}\left(\frac{\partial T}{\partial \dot{\phi}}\right) - \frac{\partial T}{\partial \phi} = 0$$

Thus, equation (38) yields

$$\left(\ddot{\theta} + \ddot{\phi}\right)\left[\phi\left(M + \frac{KR\phi}{3}\right)\right] + \left(M + \frac{KR\phi}{2}\right)\left(\dot{\phi}^2 - \dot{\theta}^2\right) = 0 \tag{41}$$

Equations (40) and (41) are solved simultaneously to obtain the transient conditions in phase I.

Phase II

In phase II the cables have completely unwound with $R\phi = L = \text{Constant}$. As shown by figure 3, the cables and weights now rotate about the fixed point A on the cylinder. Point A is chosen as the origin of the x,y coordinate system which is rotating about the origin (point O) of the X,Y coordinate system which is fixed. The weights and cables rotate about point A until they are colinear with a radius from the center of the payload. At this moment the cables and weights are considered released. The total energy for this phase is

$$E = \Sigma T = T_P + T_M + T_C \tag{42}$$

where

$$T_P = \frac{I\dot{\theta}^2}{2} \tag{43}$$

$$T_M = \sum_{i=1}^{n} \frac{M_i}{2}\left(\dot{X}_{Mi}^{\,2} + \dot{Y}_{Mi}^{\,2}\right) \tag{44}$$

Also,

$$X_{Mi} = L \sin(\theta + \phi + \alpha) + R \cos(\theta + \phi)$$

$$Y_{Mi} = -L \cos(\theta + \phi + \alpha) + R \sin(\theta + \phi)$$

which yields

$$\dot{X}_{Mi}^{\,2} + \dot{Y}_{Mi}^{\,2} = L^2(\dot{\theta} + \dot{\alpha})^2 + R^2\dot{\theta}^2 + 2RL\dot{\theta}(\dot{\theta} + \dot{\alpha})\sin\alpha \tag{45}$$

Substituting equation (45) into equation (44)

$$T_M = \sum_{i=1}^{n} \frac{M_i}{2}\left[L^2(\dot{\theta} + \dot{\alpha})^2 + R^2\dot{\theta}^2 + 2RL\dot{\theta}(\dot{\theta} + \dot{\alpha})\sin\alpha\right] \tag{46}$$

To find the energy of the cables, refer to figure 3. The location of the jth particle on the ith cable is

$$X_j = R\cos(\theta + \phi) + l\sin(\theta + \phi + \alpha)$$

$$Y_j = R\sin(\theta + \phi) - l\cos(\theta + \phi + \alpha)$$

Thus,

$$\dot{X}_j^2 + \dot{Y}_j^2 = R^2\dot{\theta}^2 + l^2(\dot{\theta} + \dot{\alpha})^2 + 2Rl\dot{\theta}(\dot{\theta} + \dot{\alpha})\sin\alpha$$

The mass of the jth particle on the ith cable is

$$dm_i = K_i\, dl$$

Then, the energy of the jth particle is

$$dT_{Ci} = \frac{K_i}{2}\left(\dot{X}_j^2 + \dot{Y}_j^2\right)dl$$

Therefore, the total kinetic energy of the cables is

$$T_C = \int_0^L \sum_{i=1}^{n} \frac{K_i}{2}\left[R^2\dot{\theta}^2 + l^2(\dot{\theta} + \dot{\alpha})^2 + 2Rl\dot{\theta}(\dot{\theta} + \dot{\alpha})\sin\alpha\right]dl$$

$$= \sum_{i=1}^{n} \frac{K_i}{2}\left[LR^2\dot{\theta}^2 + \frac{L^3(\dot{\theta} + \dot{\alpha})^2}{3} + RL^2\dot{\theta}(\dot{\theta} + \dot{\alpha})\sin\alpha\right] \qquad (47)$$

Again, let

$$\sum_{i=1}^{n} M_i = M$$

$$\sum_{i=1}^{n} K_i = K$$

Substituting equations (43), (46), and (47) into equation (42) yields

$$T = \frac{I\dot{\theta}^2}{2} + \frac{M}{2}\left[L^2(\dot{\theta} + \dot{\alpha})^2 + R^2\dot{\theta}^2 + 2RL\dot{\theta}(\dot{\theta} + \dot{\alpha})\sin\alpha\right]$$

$$+ \frac{KL}{2}\left[R^2\dot{\theta}^2 + \frac{L^2(\dot{\theta} + \dot{\alpha})^2}{3} + RL\dot{\theta}(\dot{\theta} + \dot{\alpha})\sin\alpha\right] \tag{48}$$

Equation (48) is then used in Lagrange's equations to obtain the equations of motion. Lagrange's equation for θ reduces to

$$\frac{d}{dt}\left(\frac{\partial T}{\partial \dot{\theta}}\right) - \frac{\partial T}{\partial \theta} = 0 \tag{49}$$

Performing the required operations on equation (48) as indicated by equation (49) yields

$$\left[I + R^2(M + KL) + L^2\left(M + \frac{KL}{3}\right) + 2\left(M + \frac{KL}{2}\right)RL\sin\alpha\right]\ddot{\theta}$$

$$+ \left[L^2\left(M + \frac{KL}{3}\right) + \left(M + \frac{KL}{2}\right)RL\sin\alpha\right]\ddot{\alpha} + RL\dot{\alpha}\cos\alpha\left[\left(M + \frac{KL}{2}\right)(2\dot{\theta} + \dot{\alpha})\right] = 0 \tag{50}$$

In like manner, Lagrange's equation for α reduces to

$$\frac{d}{dt}\left(\frac{\partial T}{\partial \dot{\alpha}}\right) - \frac{\partial T}{\partial \alpha} = 0 \tag{51}$$

and equation (48) becomes

$$\left[L^2\left(M + \frac{KL}{3}\right) + \left(M + \frac{KL}{2}\right)RL\sin\alpha\right]\ddot{\theta} + \left[L^2\left(M + \frac{KL}{3}\right)\right]\ddot{\alpha} - RL\dot{\theta}^2\left(M + \frac{KL}{2}\right)\cos\alpha = 0 \tag{52}$$

Equations (50) and (52) are then solved simultaneously to obtain the transient conditions in phase II.

DESCRIPTION OF APPARATUS AND TEST PROCEDURE

The test apparatus shown in figure 4 consisted of: (1) support stand, (2) test model, (3) low-friction ball bearings, (4) timer, (5) air jets, (6) relay, (7) cables, and (8) one of two weights.

The test model was an 8-inch-diameter metallic cylinder with a moment of inertia about the spin axis of 0.027 slug-feet^2. The model was mounted through the longitudinal axis on low-friction bearings, with a maximum friction torque of 0.14 inch-ounce at velocities approaching zero spin. The air jets were used to spin up the model for the test. The timer consisted of an 1,800-rpm synchronous motor with a pointer keyed directly to the motor shaft. The timer was started and high-speed motion pictures were taken of each test. From the motion pictures, the initial release of the weights was spotted, and the position of the pointer on the synchronous motor at that instant was considered zero time. The angular velocity of the model was determined at any specified time during the test by measuring a very small angular displacement of the model by use of the grid on the face of the cylinder and dividing by the corresponding incremental time, determined by the arc traveled by the timing pointer. The motion pictures were taken by a 16-millimeter camera operating at approximately 1,000 frames per second.

The initial release of the weights was by means of an electrical circuit. The circuit (fig. 5) consisted of a power supply, microswitch, insulated copper rings, and an external relay. The power supply consisted of eight silver-zinc rechargeable batteries rated at 1.8 volts each and located inside the model on the spin axis. One lead from the power supply was grounded directly to the metallic cylinder, and the other lead was connected in series with the microswitch and two copper rings. The copper rings were insulated along the inside circumference from the outside of the model. The microswitch was operated by an external relay, which forced a plunger located inside the shaft to close the switch. Initially, the weights were attached to the cylinder. When the microswitch was activated, a short circuit was created across the section of cable between points A and B shown in figure 5. The current heats this section of cable beyond its melting point and thereby releases the weights and cables which start unwinding due to centrifugal force. The other end of the cable is attached to the model. When the cables were completely unwound and in a radially outward position, the test was completed.

The cable used for this experiment was 0.010-inch-diameter music wire with a value of K equal to 1.73×10^{-5} slugs per foot. The weights were identical and had a total mass of 2.462×10^{-3} slugs. The cable length (3.0189 feet) was measured from the surface of the model to the center of gravity of the weight.

A possible mechanism that can be used to release the cables from the body when the cables are in a radially outward position is shown in figure 6. Although this mechanism was not used in the despin experiment, tests show a release to within 2° of the desired 90° release angle. Figure 7 shows a sequence of photographs taken of the release test.

ANALYSIS OF EXPERIMENTAL DATA

The moment of inertia of the model about the spin axis was determined experimentally by the compound pendulum method to within an estimated error of ±10 percent.

At a given time during the test, the weights were released and motion pictures taken at a speed of approximately 1,000 frames per second. The motion of the cylinder was analyzed by using a film viewer which had a vernier scale graduated to one-quarter of a degree. In order to obtain the time history of the angular motion, the following procedure was used. The hairline on the viewer was set on a degree mark on the face of the cylinder as seen in the viewer. The corresponding position of the pointer on the face of the motor timer was noted. The pointer on the timer moved through an arc of 90°, a period of time of 1/120 of a second. The hairline on the viewer was rotated to line up with the same degree mark on the face of the cylinder. Then the angle of rotation of the cylinder for the given time interval was read from the vernier scale. As the spin rate approached zero, the angle of rotation of the cylinder for the given time interval approached the tolerance of the vernier scale. Thus, for the lower spin rates, the time history of the despin becomes less accurate. The theoretical prediction of $\dot{\theta}$ plotted against time is compared with the experimental points in figure 8 for an inertia at the measured value and at ±10 percent of the measured value.

L 1 8 3 5

RESULTS AND DISCUSSION

The length of cable required for any spin-reduction ratio is shown to be independent of the initial spin rate. However, the accuracy of the residual spin is no better than the prediction of the initial spin after a value of λ has been selected that is not equal to zero. If the desired residual spin is zero, then the length is completely independent of the initial spin. The length varies with the parameter $\frac{I}{MR^2}$ for a constant value of KL/M and λ. The effect on λ due to an increase in the ratio of cable weight to attached weight is significant. An example of this significance is seen in figure 9. This plot shows the variation of cable length with KL/M to achieve various values of λ for a payload configuration of $\frac{I}{MR^2} = 200$. If a value of $\lambda = 0.10$ is desired, a cable length of approximately 11.83 feet is needed if the cable weight is considered negligible and R is assumed to be 1 foot. However, if the cable weight is one-half the weight of the attached masses and the same cable length is used, then a value of λ of approximately 0.019 is achieved as seen from the plot in figure 9 of λ against KL/M.

Investigation of the error in residual spin due to errors in the physical constants of moment of inertia about roll axis and cable length shows the largest error is from the measured inertia. This error due to the expected error from measuring the inertia is greater than that for the length. The error in residual spin (within ±5 percent for all the cases considered) is shown plotted against the error in inertia in figure 10. The positive values of $\Delta I/I$ correspond to inertias that were measured lower than the actual inertia and the negative values of $\Delta I/I$ correspond to inertias that were measured higher than the actual inertia. When the inertia is measured too high, the corresponding cable length is too long for a given case. If the desired λ is at or near zero, this error can produce a residual spin opposite in sense to the initial spin. The slope of the curve in figure 10 is approximately 1:200 so that an error of 5 percent in inertia produces an error of $\Delta\lambda \approx 2.5 \times 10^{-2}$, where $\Delta\lambda = \lambda_a - \lambda_d$.

Figure 11 shows the error in residual spin plotted against $\frac{I}{MR^2}$ for an error of ±0.25 percent in length of cable and for various ratios of cable weight to attached weight (KL/M) and spin-reduction ratios (λ). The error in residual spin is shown to decrease as λ is increased.

Examination of the transient conditions reveals that an increase in the parameter $\frac{I}{MR^2}$ results in a decrease in the error in the residual spin due to a release of the cables and weights at an angle $\alpha \neq 90^\circ$. Figure 12 shows the error in the residual spin due to a release of the weights and cables at an error in release of $\Delta\alpha = \pm 20^\circ$ from $\alpha = 90^\circ$. This error is shown plotted against $\frac{I}{MR^2}$ for various values of KL/M and is less than 0.01 for most cases considered. The decrease in error with an increase in $\frac{I}{MR^2}$ is due to a reduced slope of $\dot{\theta}$ against α as α approaches 90°. This decrease in error is also achieved with lighter cables. The quick-release mechanism in figure 6 can achieve a release within $\Delta\alpha = 2^\circ$. This type of mechanism should relegate this source of error insignificant.

The effects of all the previous errors discussed can be minimized by proper staging. An example of this staging would be to reduce the large initial spin rate to an intermediate fraction of the desired reduction value. The second stage of despin would then have the final spin rate of the first stage as its initial spin rate. Therefore, for any error in the physical constants or in the release angle, the total error produced on the residual spin is substantially reduced. Care must be exercised when the first-stage spin reduction is close to zero. The

tolerance on this reduction can produce a spin in the opposite sense for the second stage. This type of spin would result in an undesirable perturbation.

The maximum deceleration experienced by a payload is seen in figure 13 for various values of $\dot{\theta}_o$ and KL/M. It is seen that the use of lighter attached masses and lower initial spin rates reduces the maximum deceleration experienced by the payload. Where noticeable, the effect of λ on the maximum deceleration is indicated in the figure. The variation of maximum deceleration with λ is explained by the fact that when the length of cable is shortened to achieve a λ for constant initial conditions, the mass of the cable is effectively increased in order to keep KL/M constant. This increase in cable mass increases the total effective mass acting to decelerate the payload; thus, there is a larger resulting deceleration. For the case of $\frac{KL}{M} = 0$, this effect is not seen. The effect of maintaining the density of the cable constant while shortening the cable length in order to achieve $\lambda \neq 0$ is seen in figure 14. This figure shows the time history of the deceleration through phases I and II on a payload with $\frac{I}{MR^2} = 100$ and $\dot{\theta}_o = 700$ rpm. For different values of λ, the payload experiences the same peak deceleration until the time of transition from phase I to phase II occurs near the time of maximum deceleration. At this time, it is possible for the maximum deceleration to occur during phase II. An extreme case of $\lambda = 0.675$ is shown to have a lower maximum deceleration and to occur before the maximum deceleration of the other values of λ. This fact can be utilized to lower the value of maximum deceleration experienced by a payload for a given set of initial conditions by despinning in two stages. The first stage would despin to a value of λ, with a transition from phase I to phase II occurring before the maximum deceleration. The residual spin from this stage is then the initial spin for the second stage.

The time required to despin for any value of λ and given initial conditions is inversely proportional to the initial spin; therefore,

$$t\dot{\theta}_o = \text{Constant}$$

As the length of cable is increased, the time required to despin to the desired λ is also increased. This time is approximated in the following manner. The results of investigating the transient conditions indicate that, in phase I, the rate $\dot{\phi}$ of the cable unwinding is almost a constant value equal to the initial spin rate. The total rate of rotation relative to the fixed coordinate system is considered constant and approximately equal to the initial spin rate. Therefore, the total number of radians traveled relative to the fixed coordinate system for

a given configuration is considered equal to the total angle in phase I plus the angle traveled in phase II; that is,

$$t\dot{\theta}_o = \frac{L}{R} + \arctan \frac{L}{R}$$

This expression yields the total time required to despin to within 0.5 percent of the actual values with L either chosen or computed for a given configuration.

The ability of the cable to withstand the expected tensile stress is a design consideration that will determine a value of KL/M. The maximum tension on the cable may occur in phase I or in phase II and, in some cases, it may occur near or at $\alpha = 90^o$. The maximum cable tension $F_{max} \frac{nRt^2}{I}$ is shown plotted against $\frac{I}{MR^2}$ in figure 15 for various values of λ and KL/M. This tension is for one of n cables of equal density and symmetrically spaced around the circumference.

Figure 8 shows the time history of the angular motion for an initial speed of 29.2 radians per second. The center curve shows the time history using the moment of inertia as determined experimentally by the compound-pendulum method. The top curve shows the time history with an increase in the moment of inertia of 10 percent and the bottom curve shows the time history with a decrease in the moment of inertia of 10 percent. The experimental data are shown to follow the theoretical prediction of the transient conditions within the limits of the apparatus.

CONCLUSIONS

The equations of motion derived for the despinning of a rigid body by utilizing weights on the ends of unwinding flexible cables show the following conclusions:

1. The length of cable of given density or mass of attached weights may be found from the initial and final angular momentum and energy equations to produce any desired spin-reduction ratio for a spinning body of known inertia and no friction.

2. The length of cable or mass used to despin a given body is a function of the spin-reduction ratio and is independent of initial spin rate. The accuracy of desired residual spin is directly dependent on the initial spin.

3. The error in the spin-reduction ratio due to an error in length of cable or measured inertia may be predicted, with the largest error produced by the large expected error in inertia.

4. In order to obtain accurate results, the weight of the cable must be considered.

5. The error in the residual spin due to a release of the cables and weights at an error in release angle of $\pm 20^{\circ}$ from the desired angle of 90° is less than 0.01 for most cases considered. This error can be made negligible by a properly designed release mechanism. This error is also reduced by using lighter cables and a higher ratio of payload inertia to initial inertia of attached masses $\frac{I}{MR^2}$ which corresponds to lighter attached weights.

6. Greater accuracy in residual spin can be obtained by proper staging of the total despin reduction.

7. The maximum payload deceleration and the maximum cable tension can occur in either first or second phase. The maximum deceleration and tension can be decreased by:

(a) Lower initial spin rate

(b) Higher value of $\frac{I}{MR^2}$

(c) Staging the despin operation so that the maximum decleration for the first stage occurs before the maximum deceleration for the configuration.

8. An expression for the total time required to despin to any residual spin rate is presented as a function of the cable length. This time is within 0.5 percent of the actual time required.

Langley Research Center,
National Aeronautics and Space Administration,
Langley Air Force Base, Va., November 1, 1961.

REFERENCES

1. Gillespie, Warren, Jr., Eide, Donald G., and Churgin, Allan B.: Some Notes on Attitude Control of Earth Satellite Vehicles. NASA TN D-40, 1959.

2. Creech, Merl D., and Fergin, Richard K.: New Mechanism Stops Spin of Rotating Masses. Product Engineering, vol. 32, no. 14, Apr. 3, 1961, pp. 56-59.

3. Fedor, J. V.: Theory and Design Curves for a Yo-Yo De-Spin Mechanism for Satellites. NASA TN D-708, 1961.

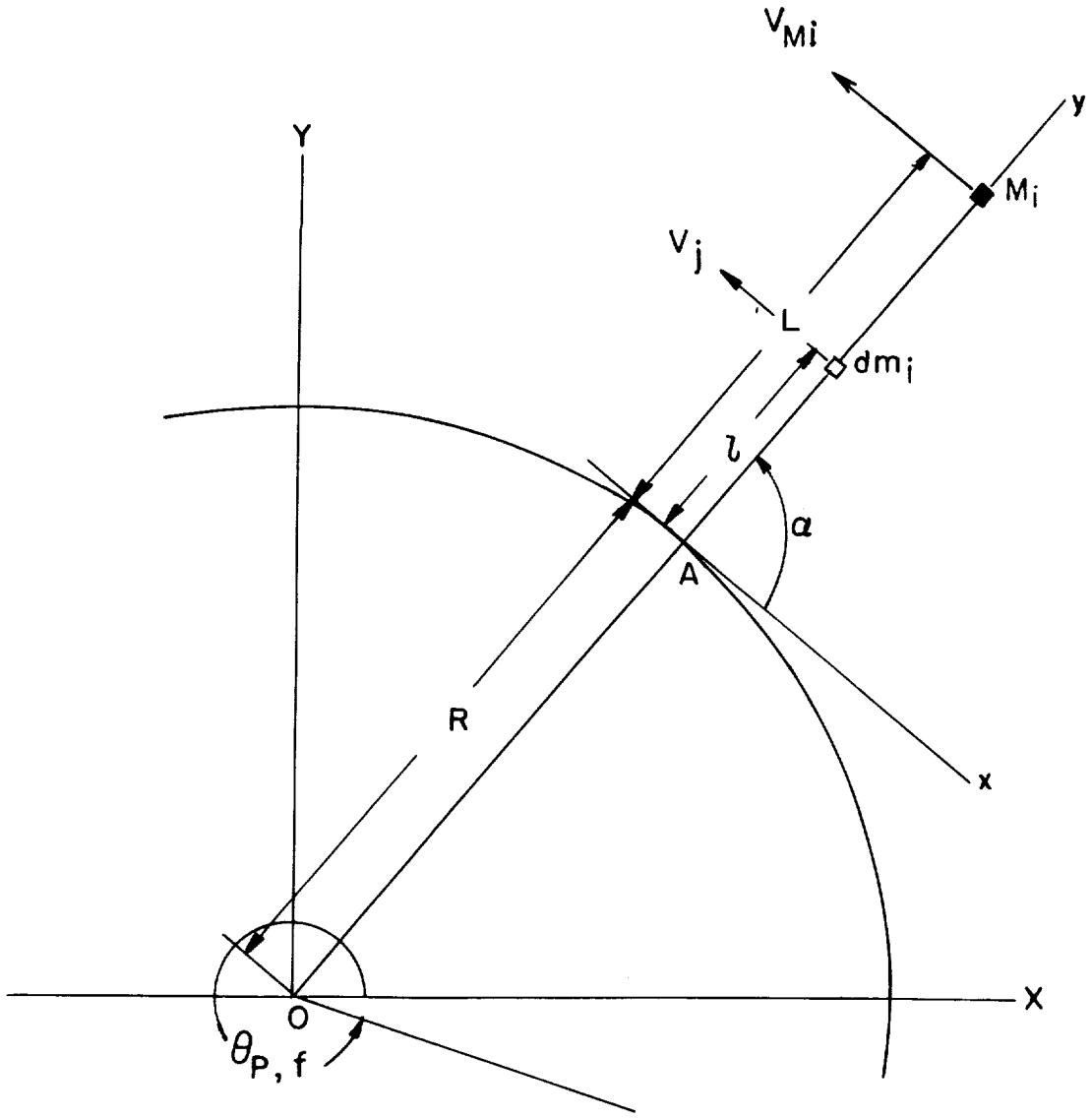

Figure 1.- Instant of release of weights and cables at $\alpha = 90^{\circ}$.

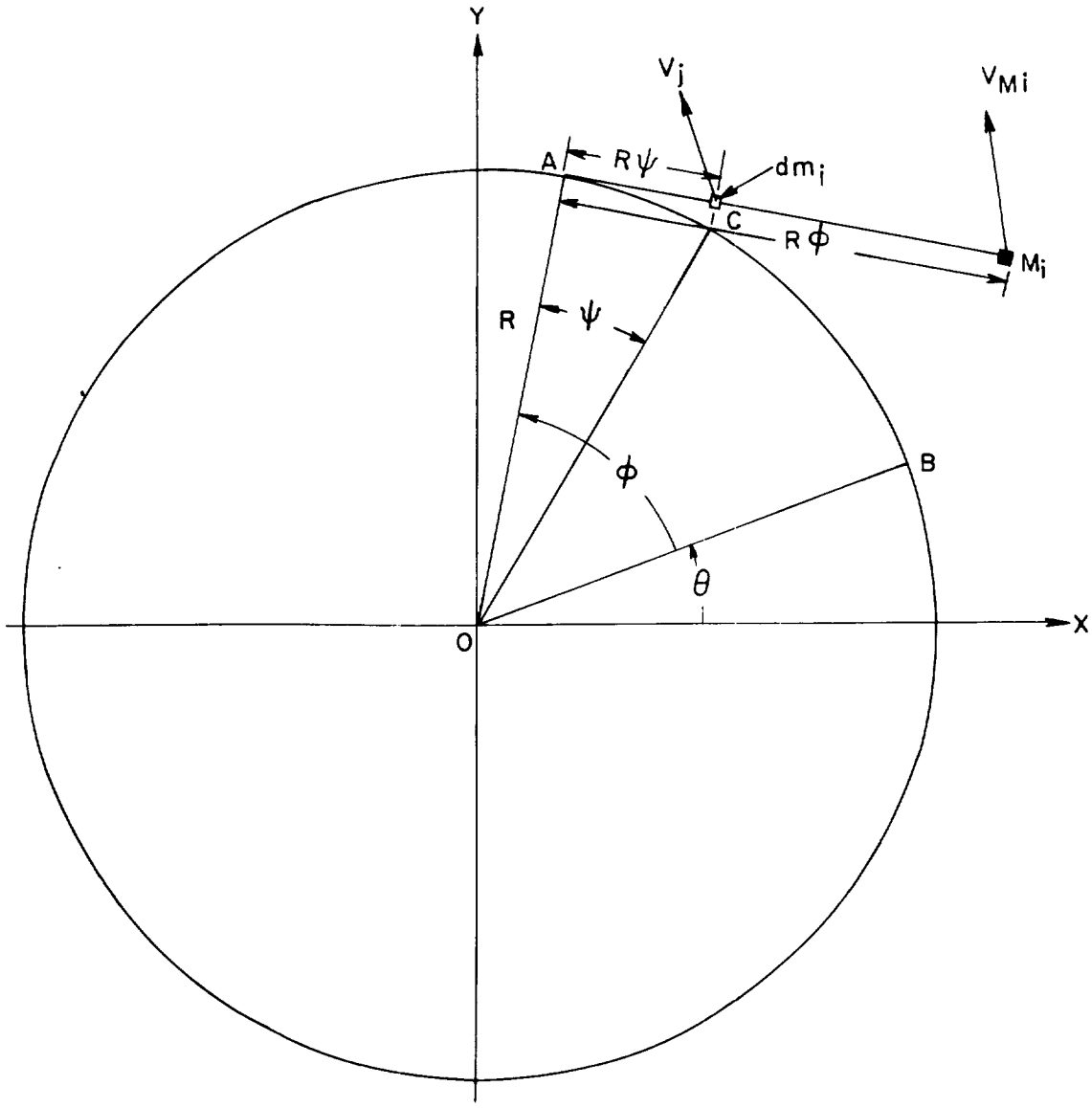

Figure 2.- Motion during phase I.

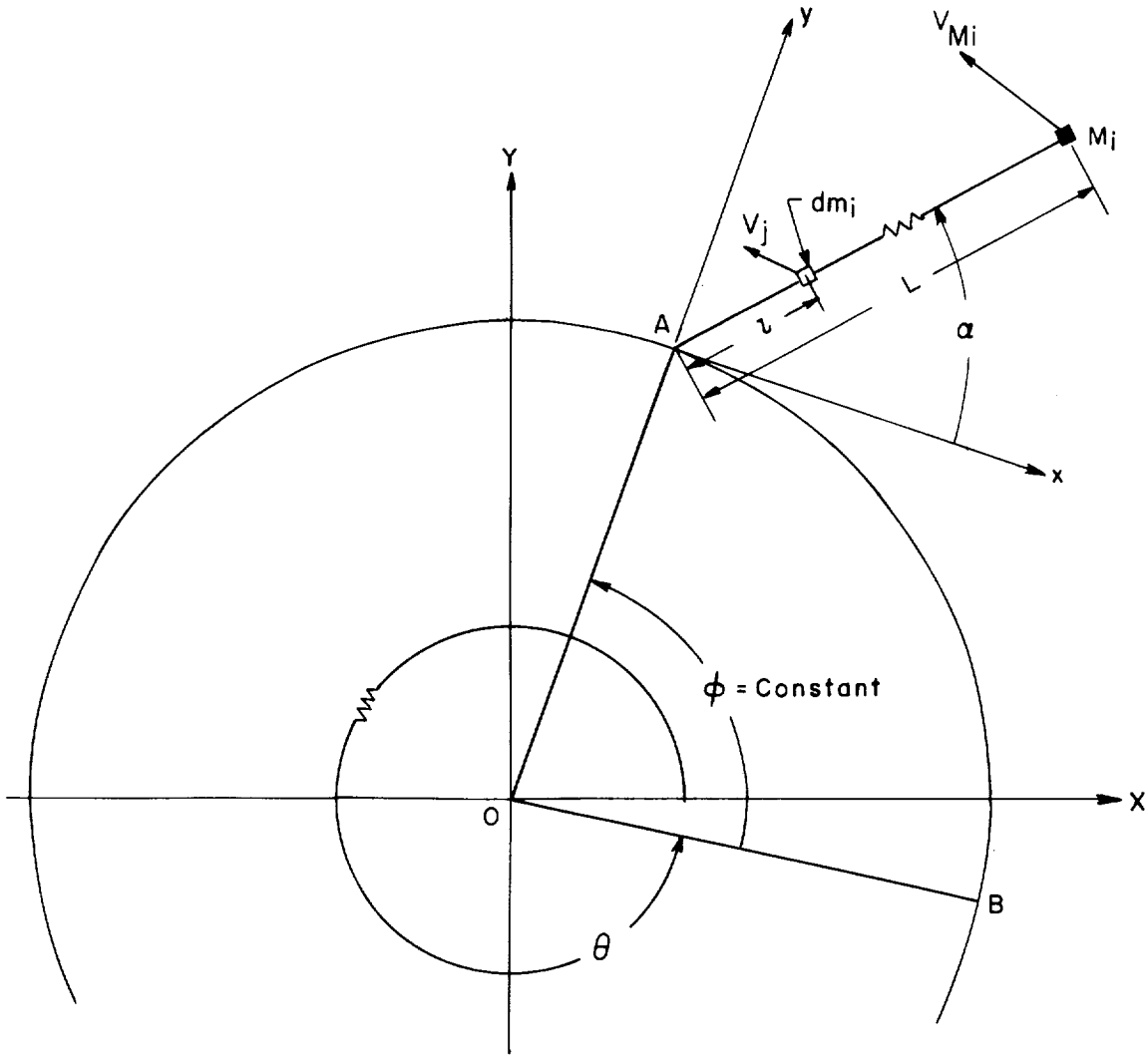

Figure 3.- Motion during phase II.

1. Support stand
2. Test model
3. Ball bearings
4. Timer
5. Air jets
6. Relay
7. Cables
8. Weight

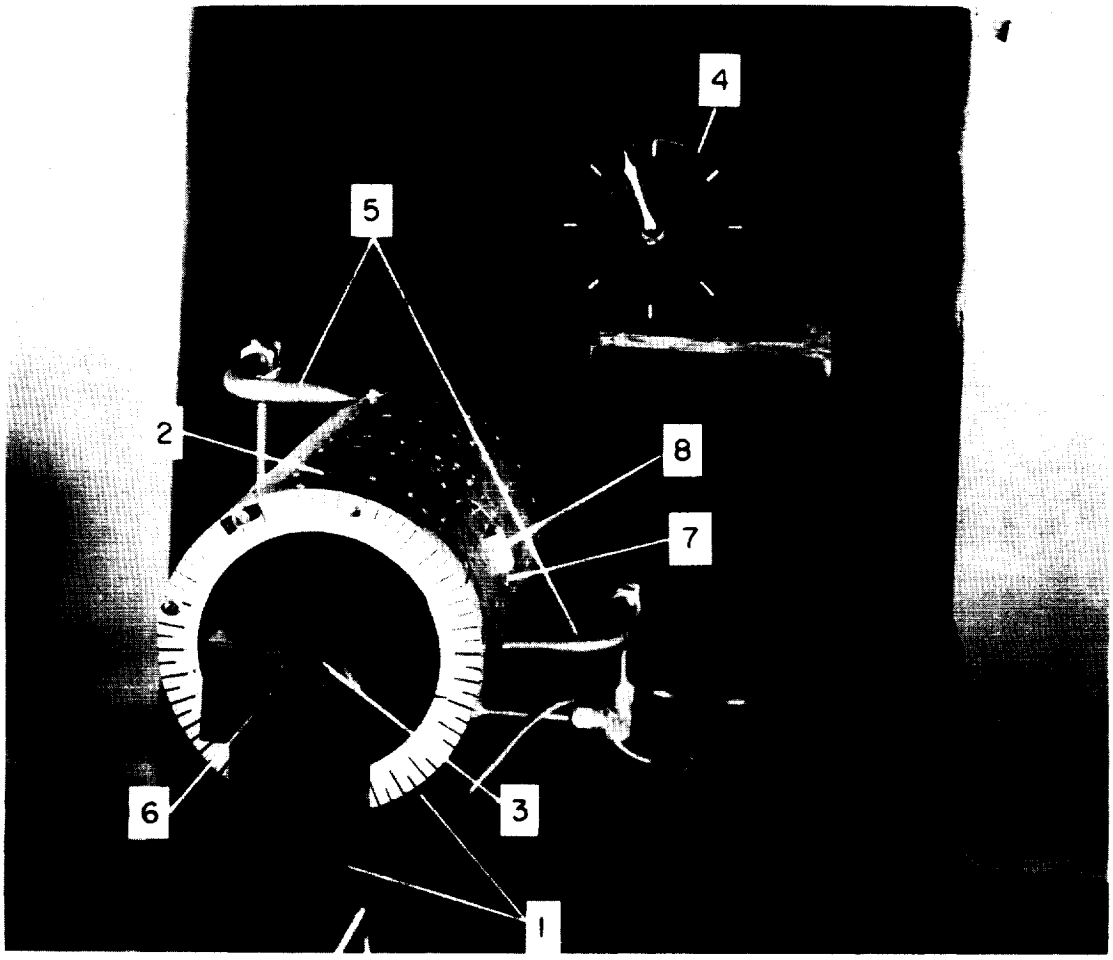

Figure 4.- Photograph of test apparatus. L-60-4903.1

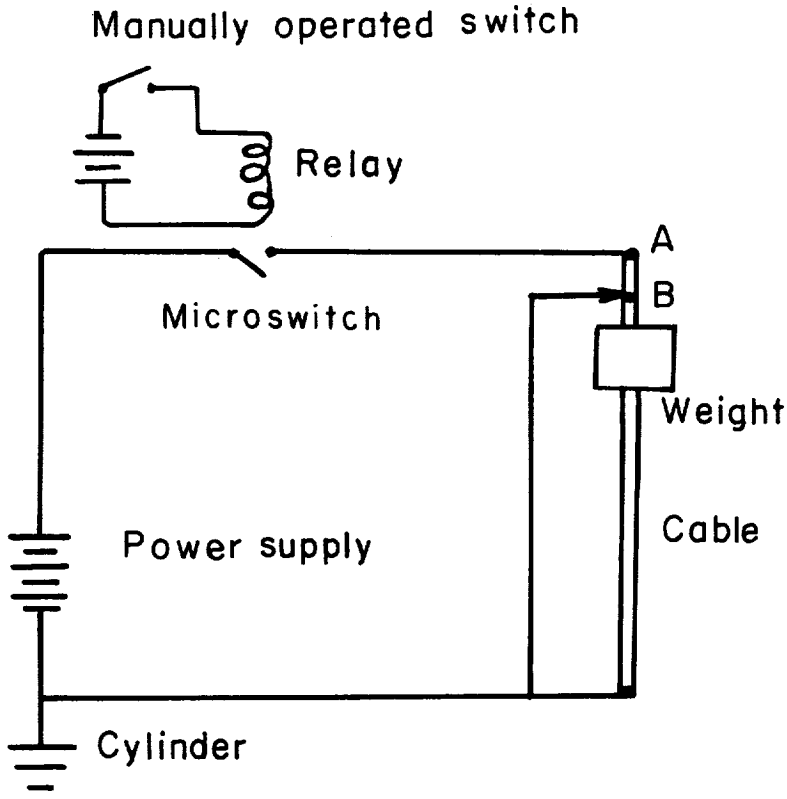

Figure 5.- Electric circuit for initial release of cables and weights.

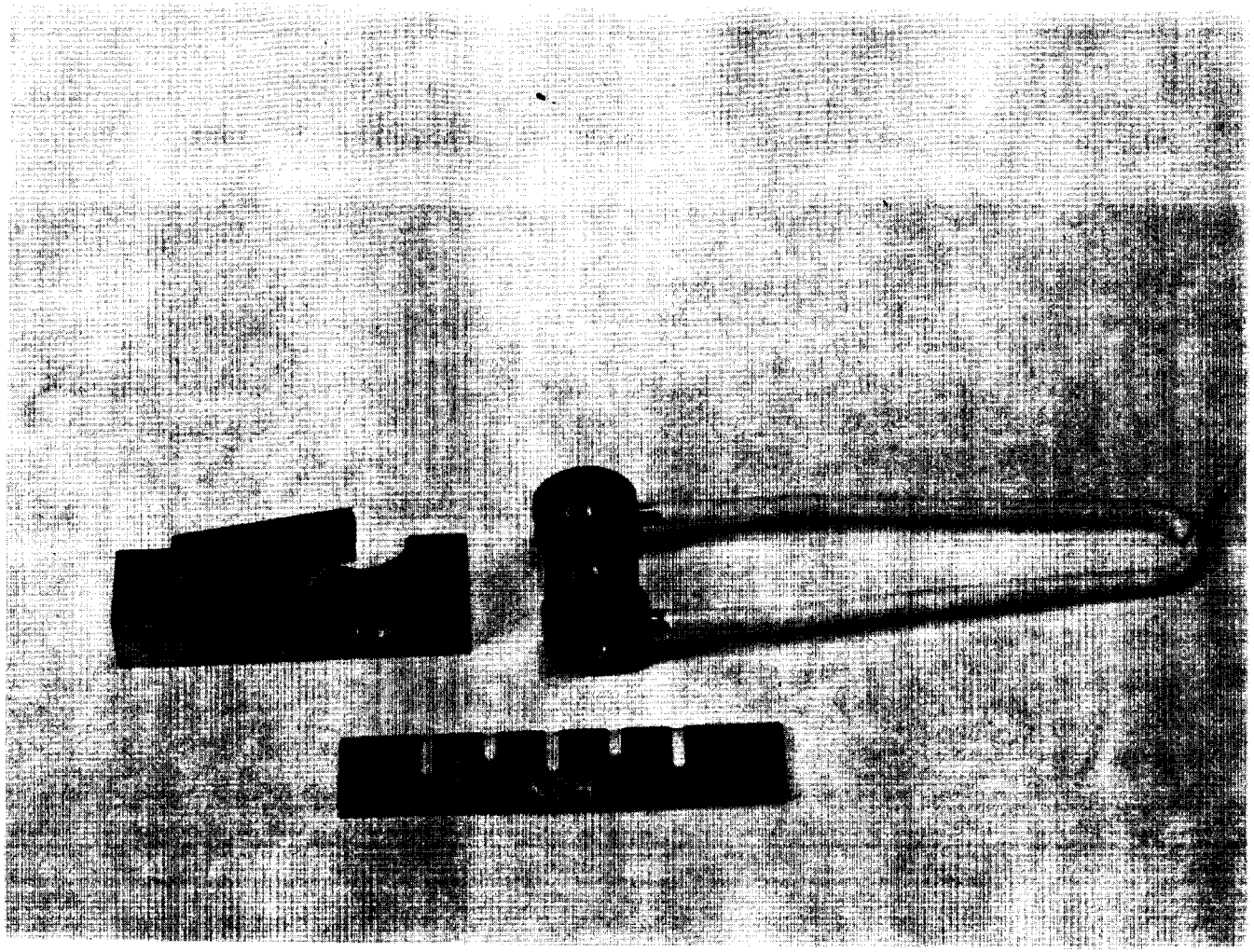

Figure 6.- Photograph of mechanism for releasing the cables. L-61-5285

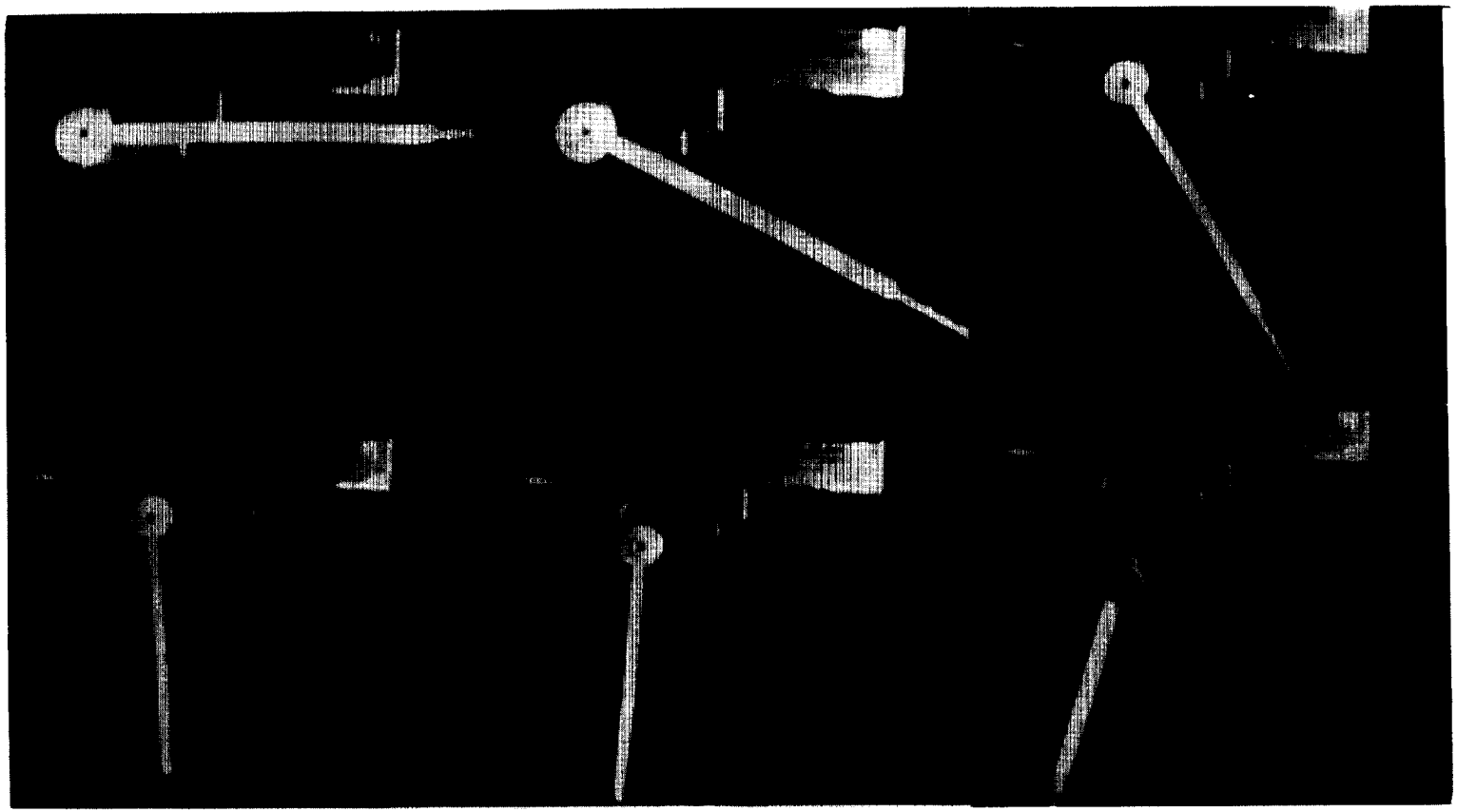

Figure 7.- Sequence of photographs of the release test. L-61-7712

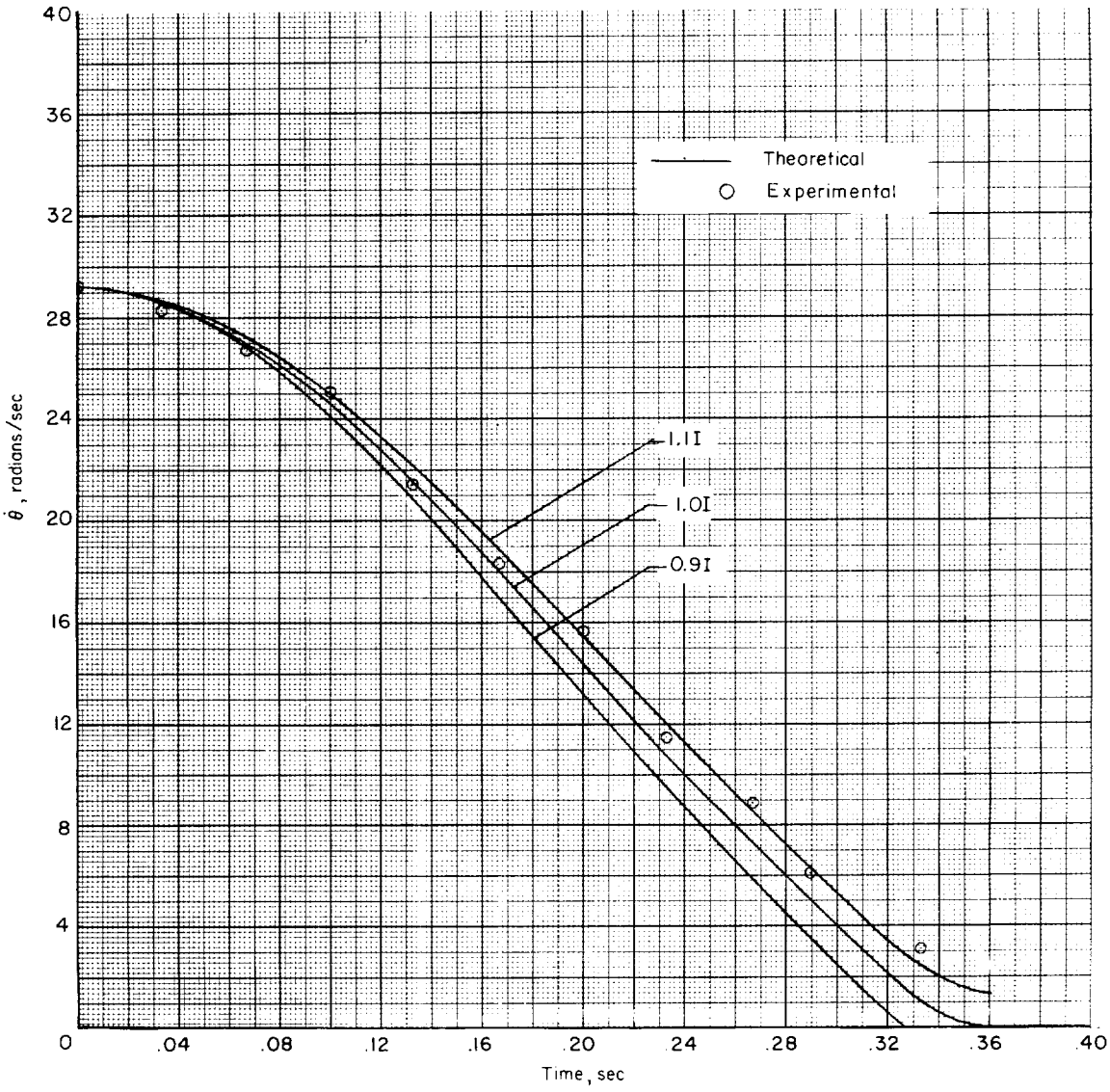

Figure 8.- Comparison of theoretical and experimental spin rate plotted against time. $\frac{I}{MR^2} = 100.16$; $\frac{KL}{M} = 0.0216$.

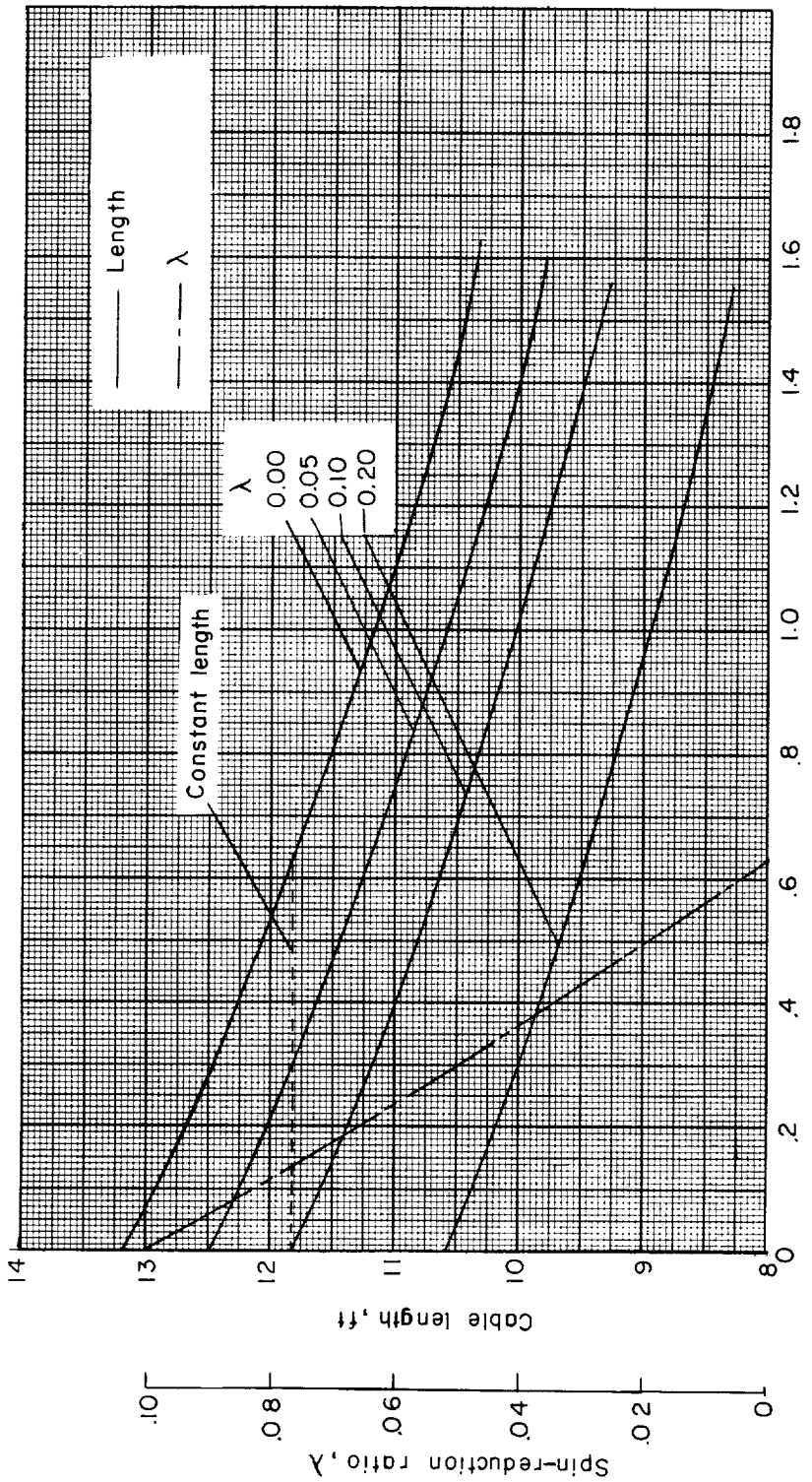

Figure 9.- Cable length and spin-reduction ratio plotted against ratio of cable weight to attached weight. $\frac{I}{MR^2} = 200$; R = 1 foot.

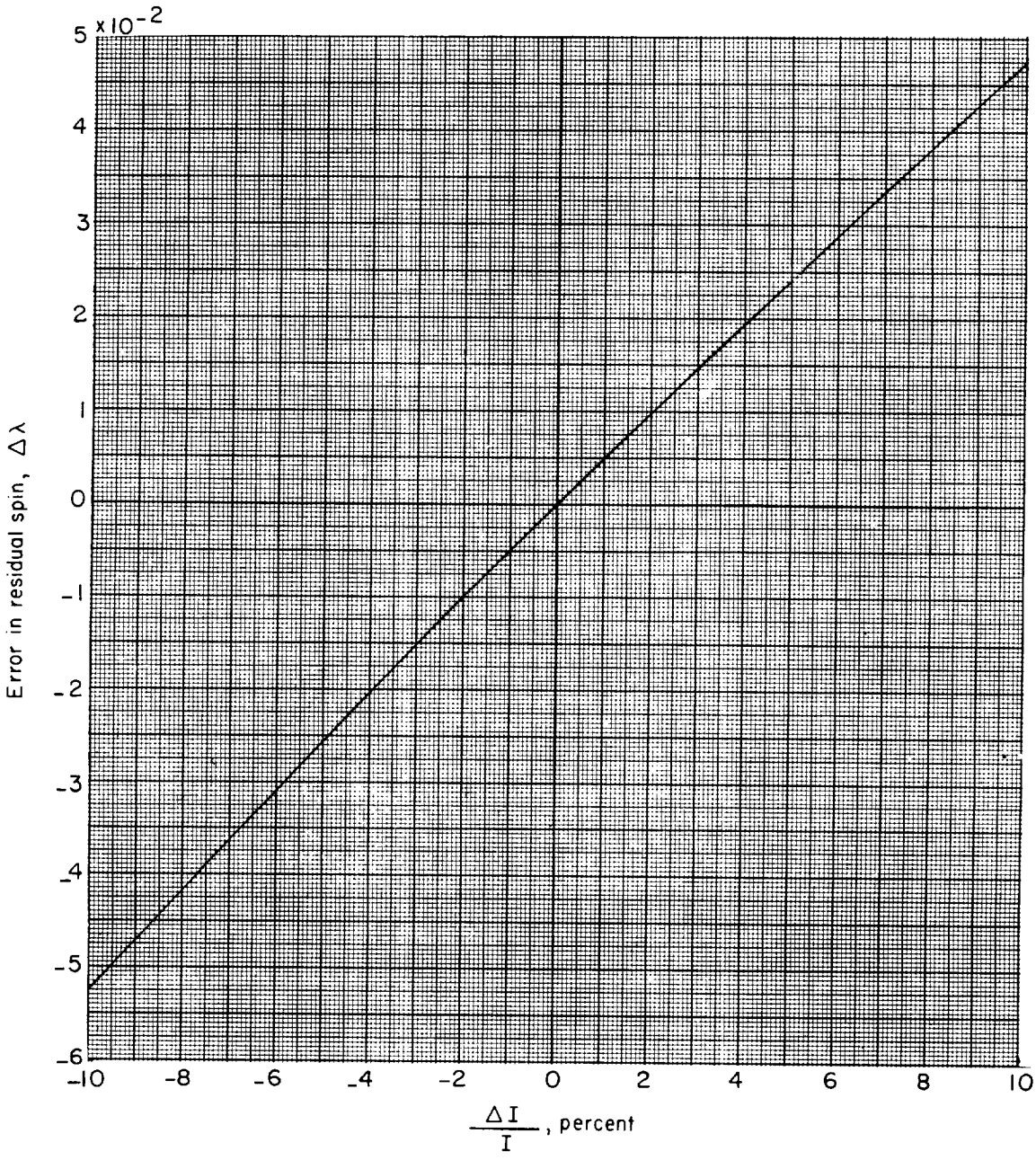

Figure 10.- Error in residual spin plotted against error in moment of inertia.

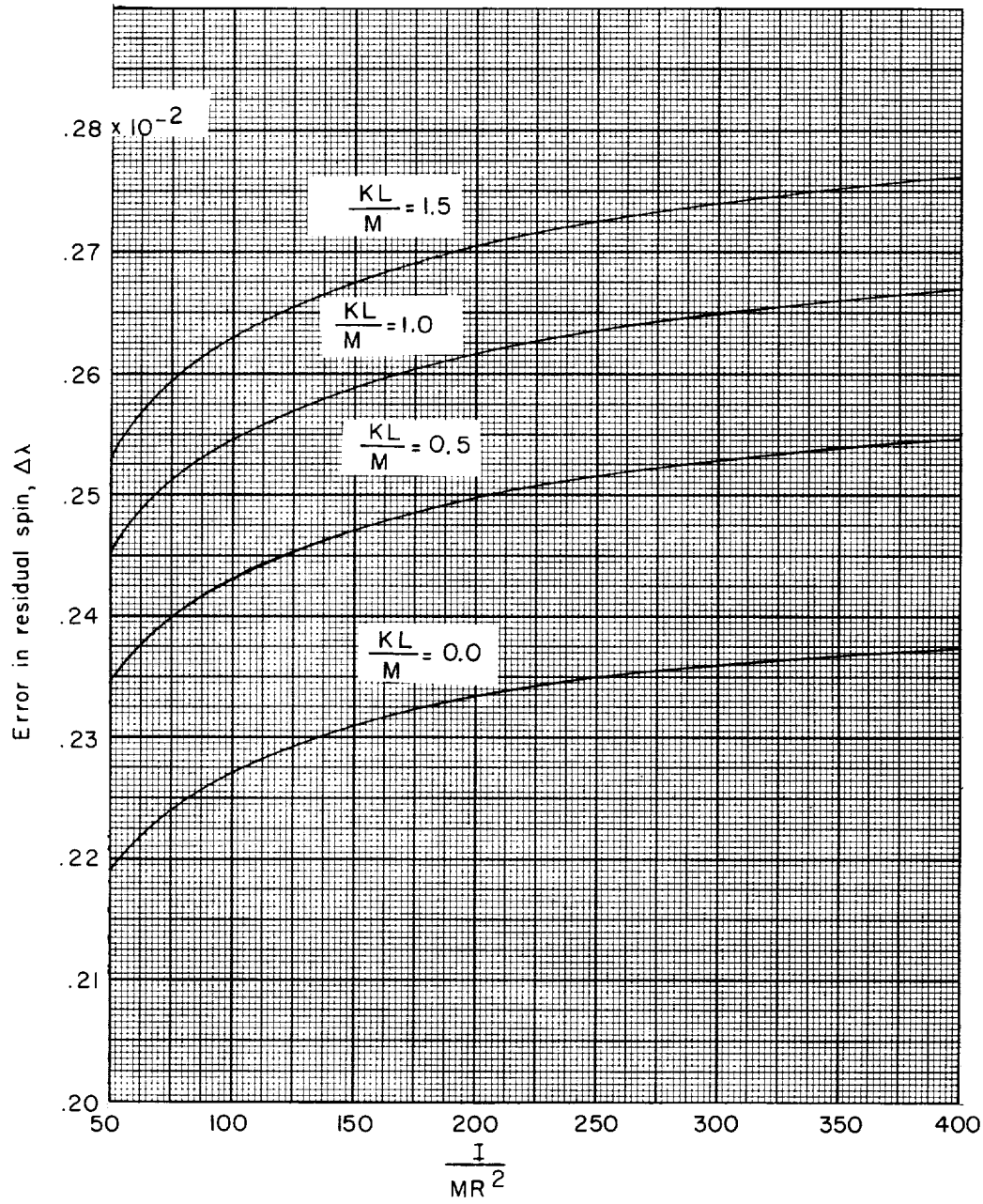

(a) $\lambda = 0.00$.

Figure 11.- Error in residual spin due to $\frac{\Delta L}{L} = \pm 0.25$ percent plotted against $\frac{I}{MR^2}$ for various values of $\frac{KL}{M}$ and λ.

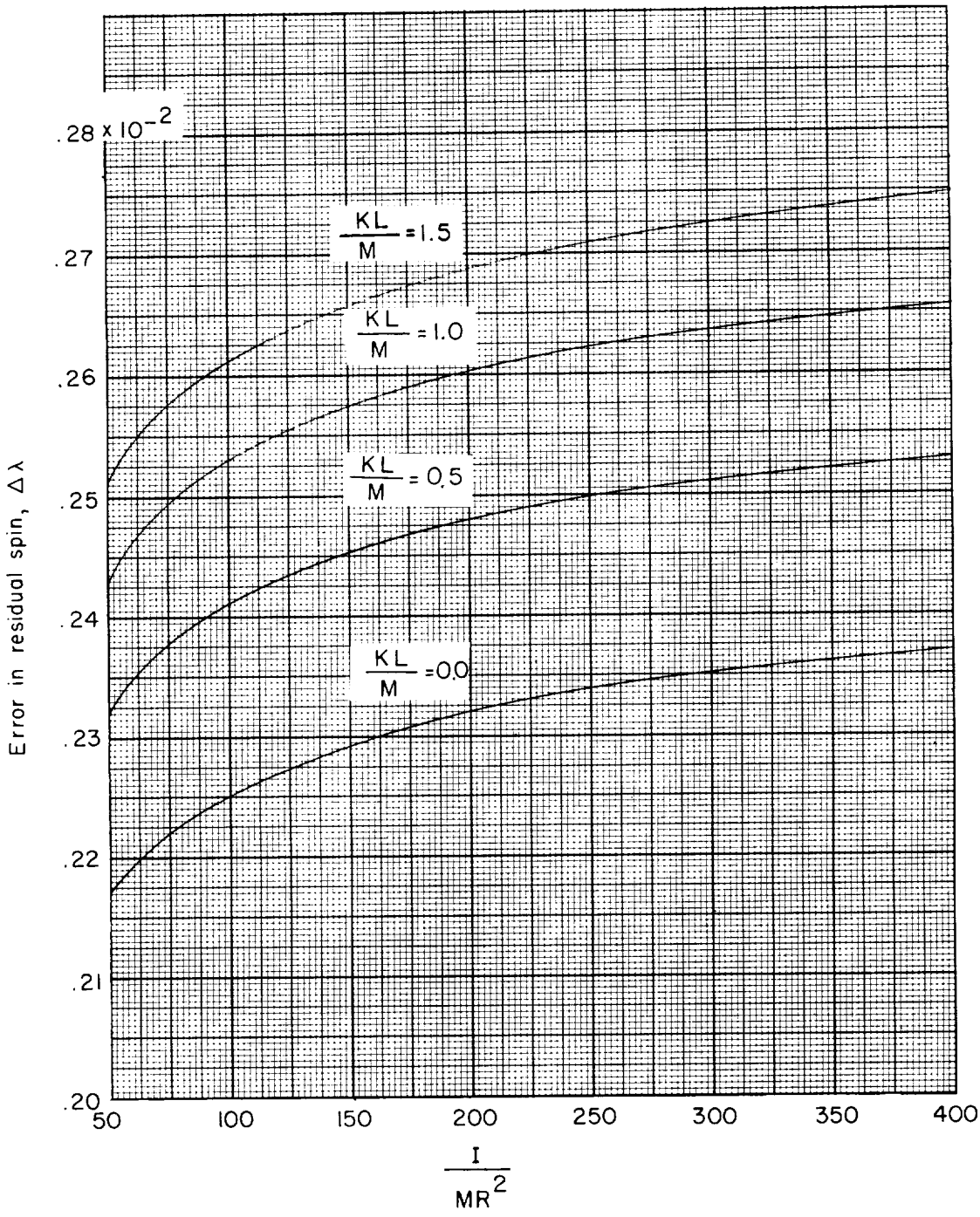

(b) $\lambda = 0.05$.

Figure 11.- Continued.

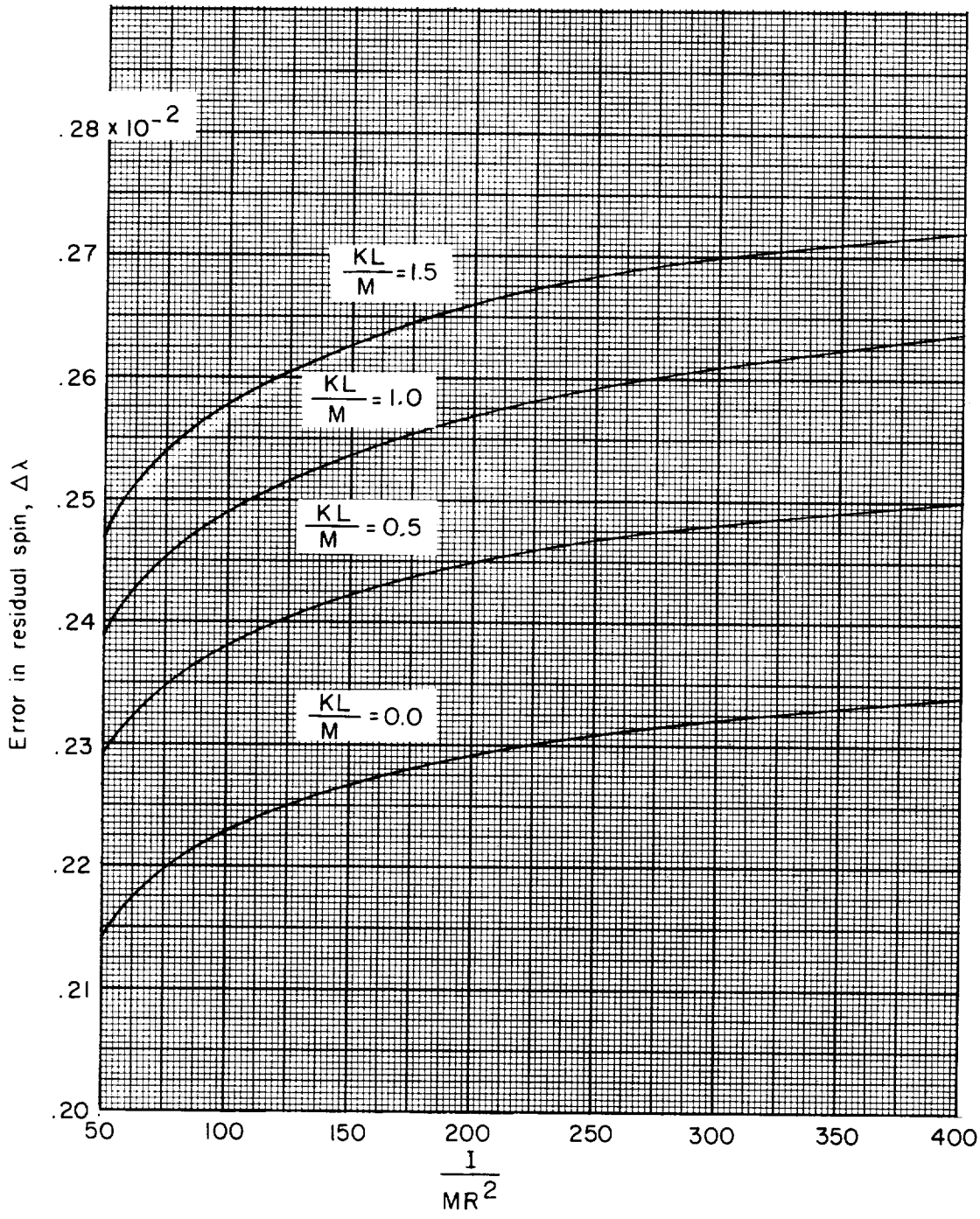

(c) $\lambda = 0.10$.

Figure 11. - Continued.

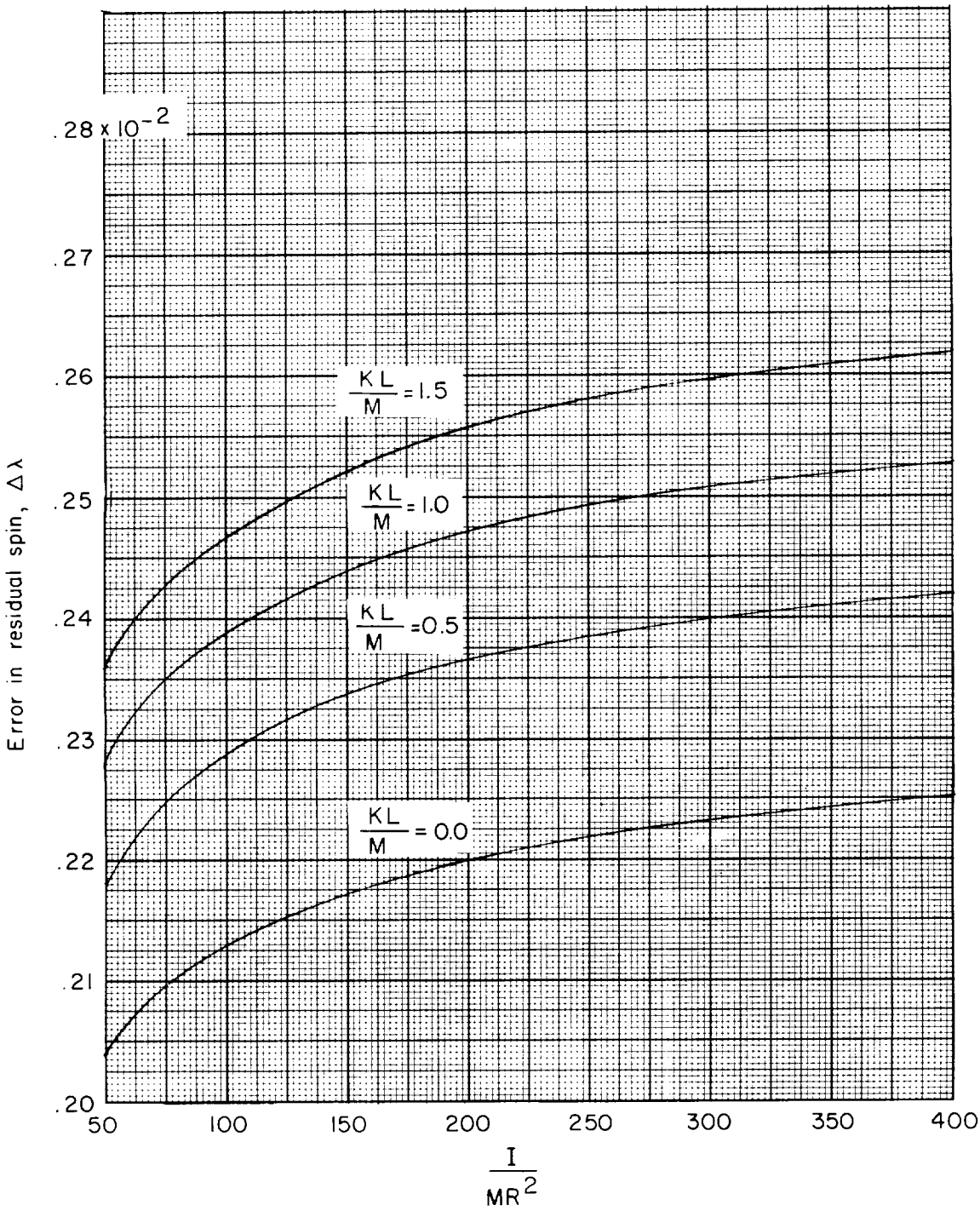

(d) $\lambda = 0.20$.

Figure 11.- Concluded.

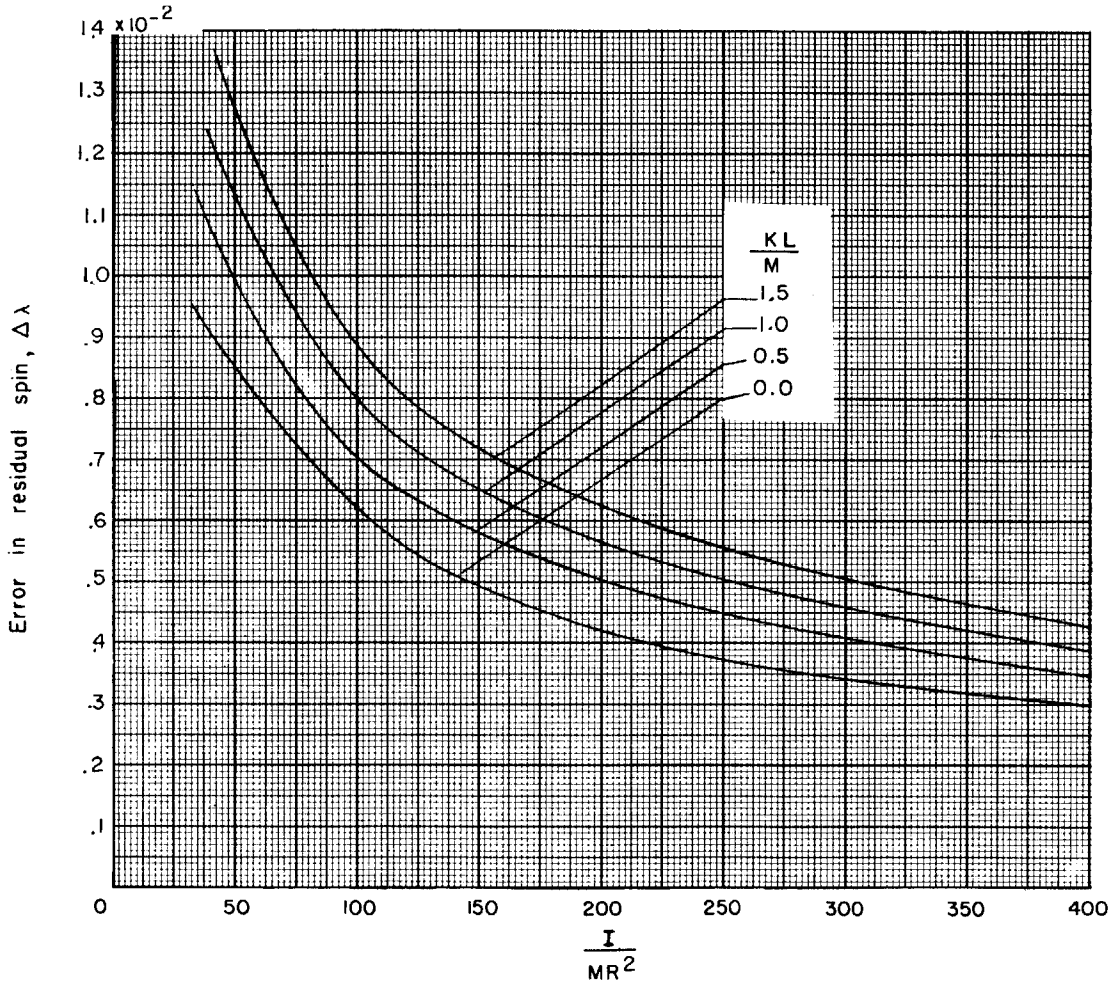

Figure 12.- Error in residual spin plotted against $\frac{I}{MR^2}$ for an error in cable release of $\Delta\alpha = \pm 20^{\circ}$ from $\alpha = 90^{\circ}$.

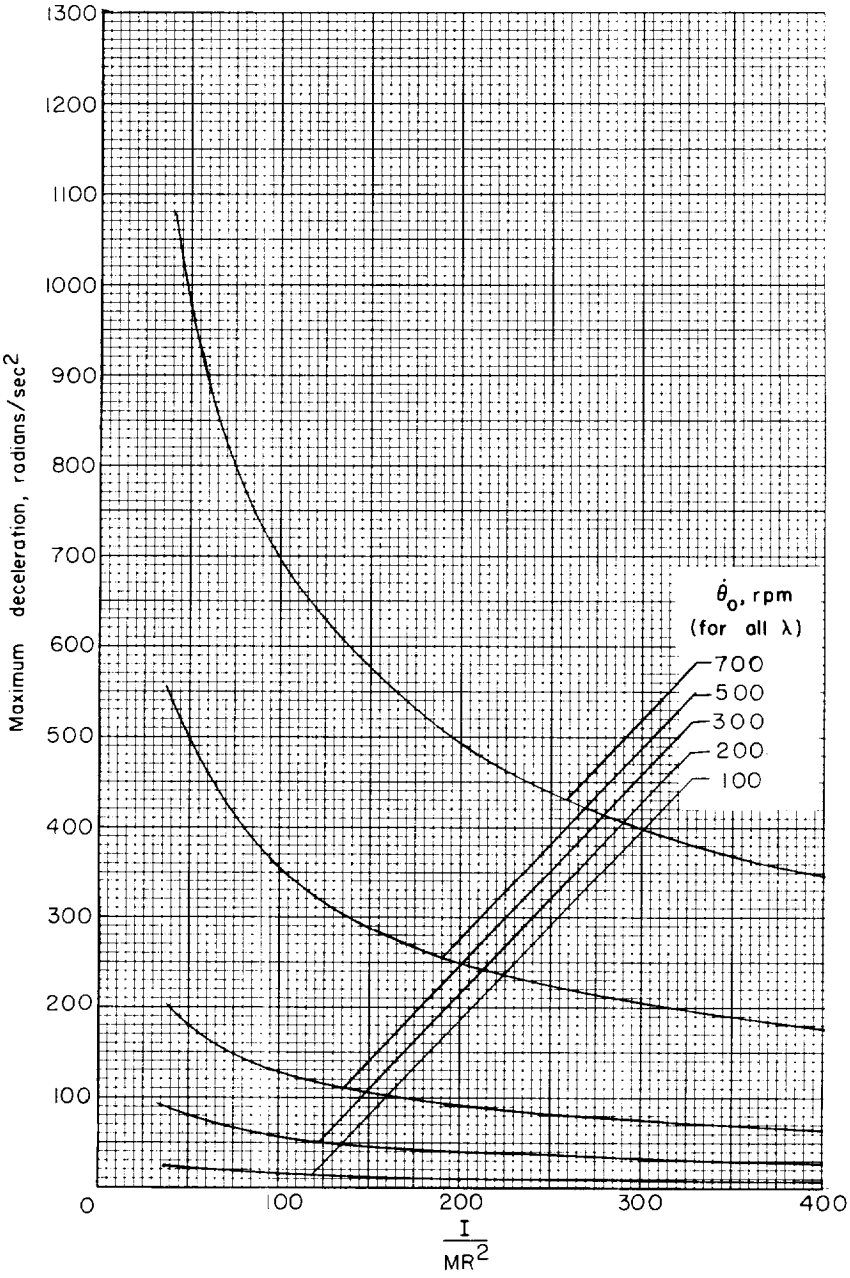

(a) $\frac{KL}{M} = 0.0$.

Figure 13.- Maximum payload deceleration plotted against $\frac{I}{MR^2}$ for various values of $\frac{KL}{M}$ and $\dot{\theta}_o$.

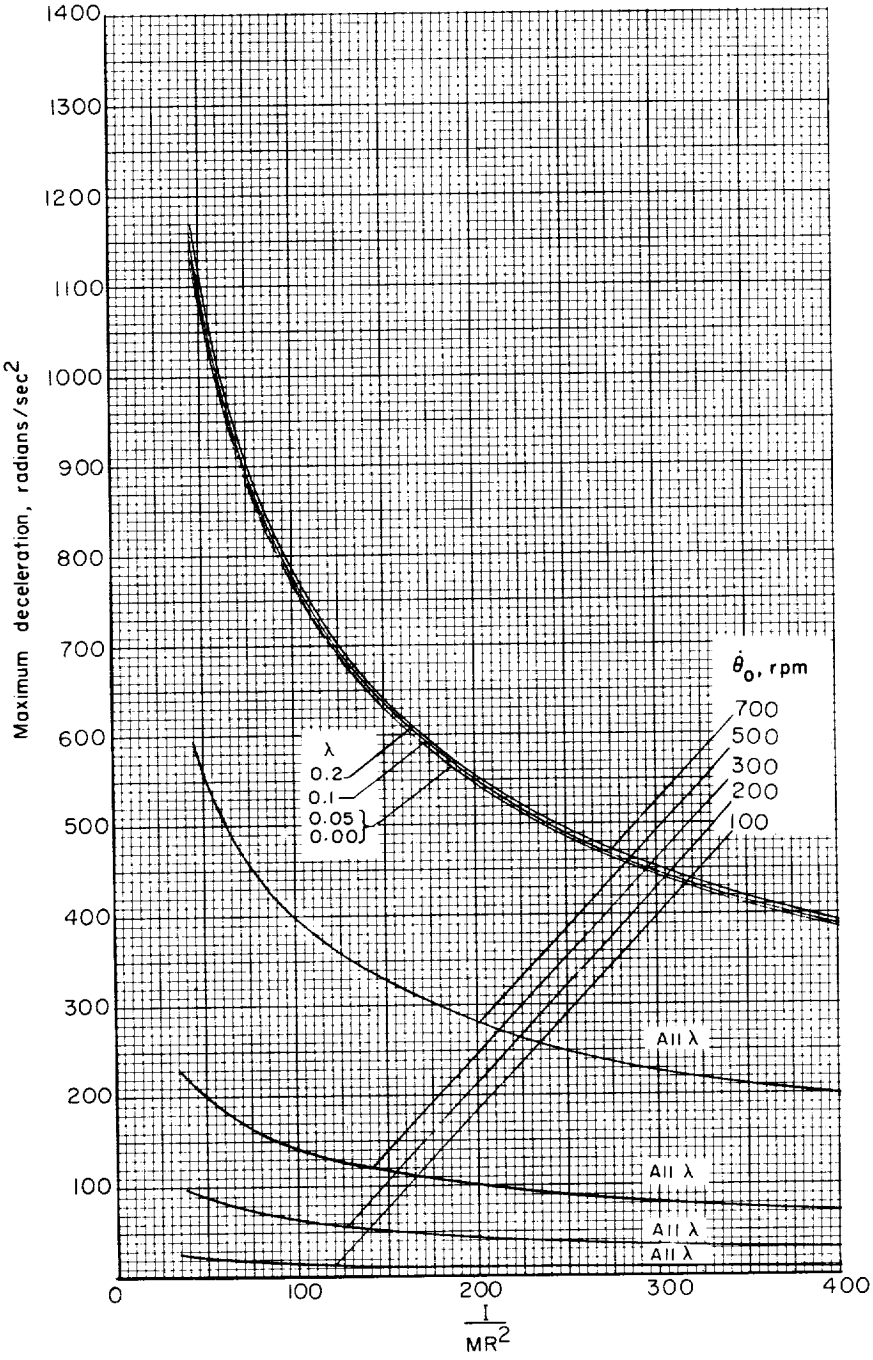

(b) $\frac{KL}{M} = 0.5$.

Figure 13.- Continued.

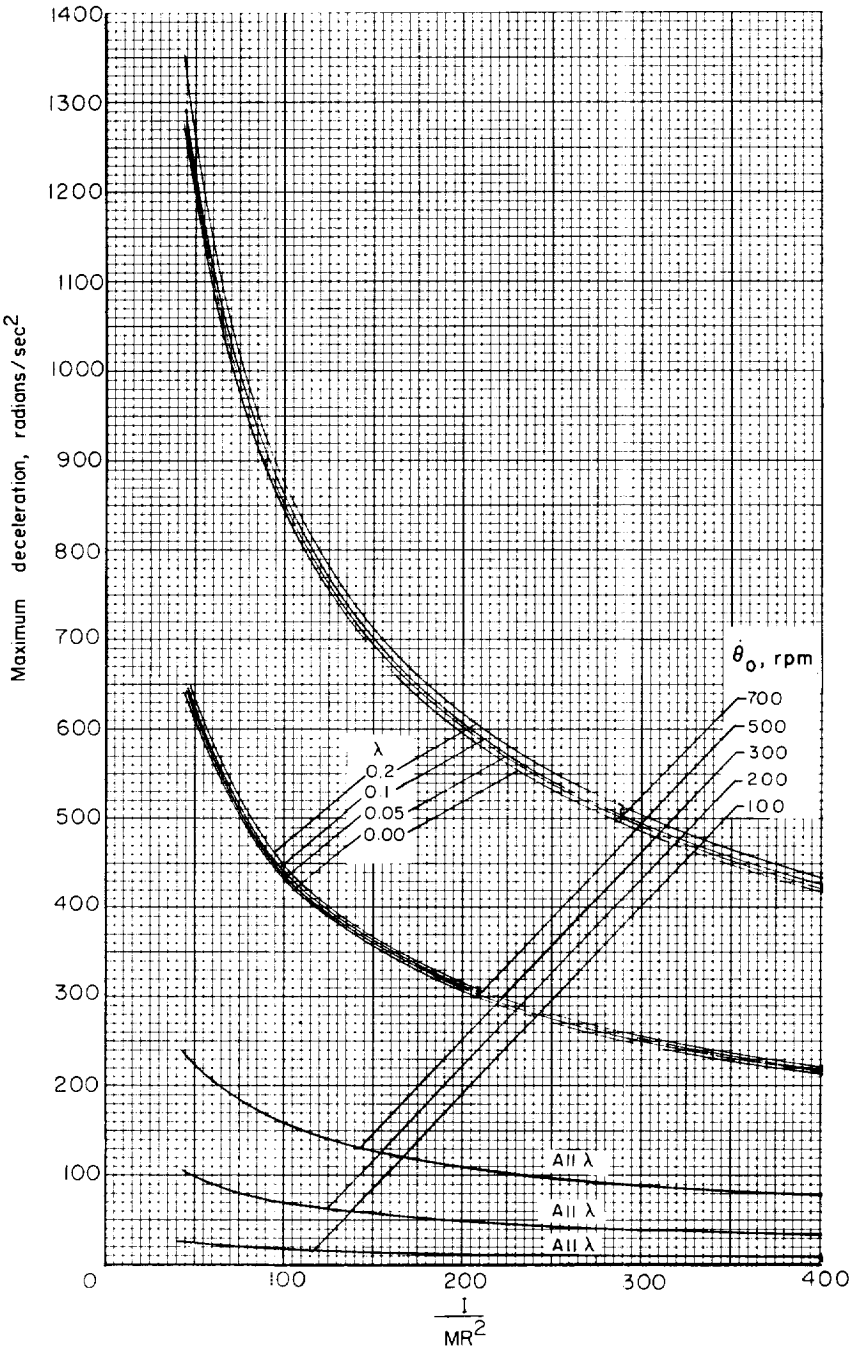

(c) $\frac{KL}{M} = 1.0$.

Figure 13.- Continued.

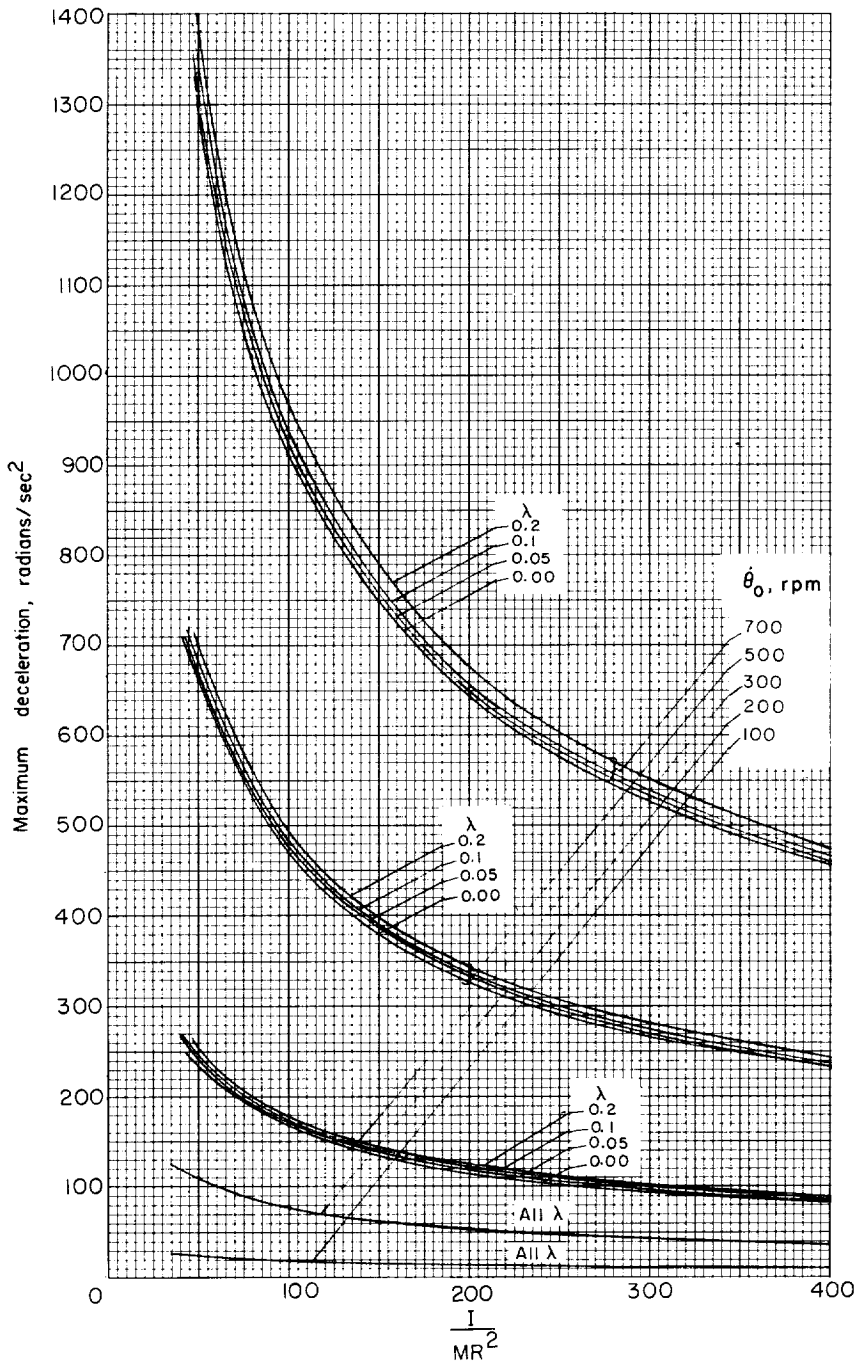

(d) $\frac{KL}{M} = 1.5$.

Figure 13.- Concluded.

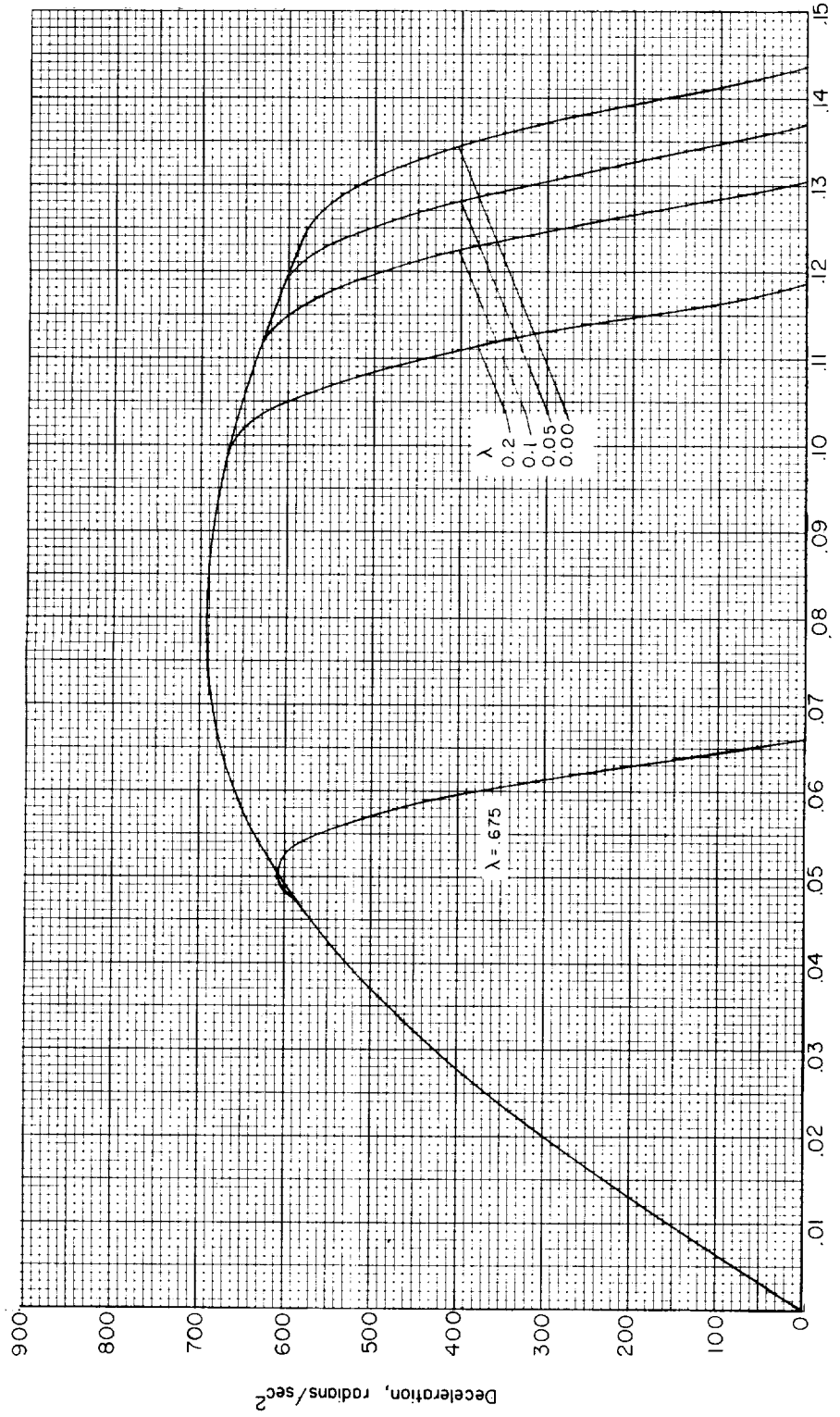

Figure 14.- Payload deceleration plotted against time at various spin-reduction ratios.

$$\frac{I}{MR^2} = 100; \quad \frac{KL}{M} = 0; \quad \dot{\theta}_o = 700 \text{ rpm}.$$

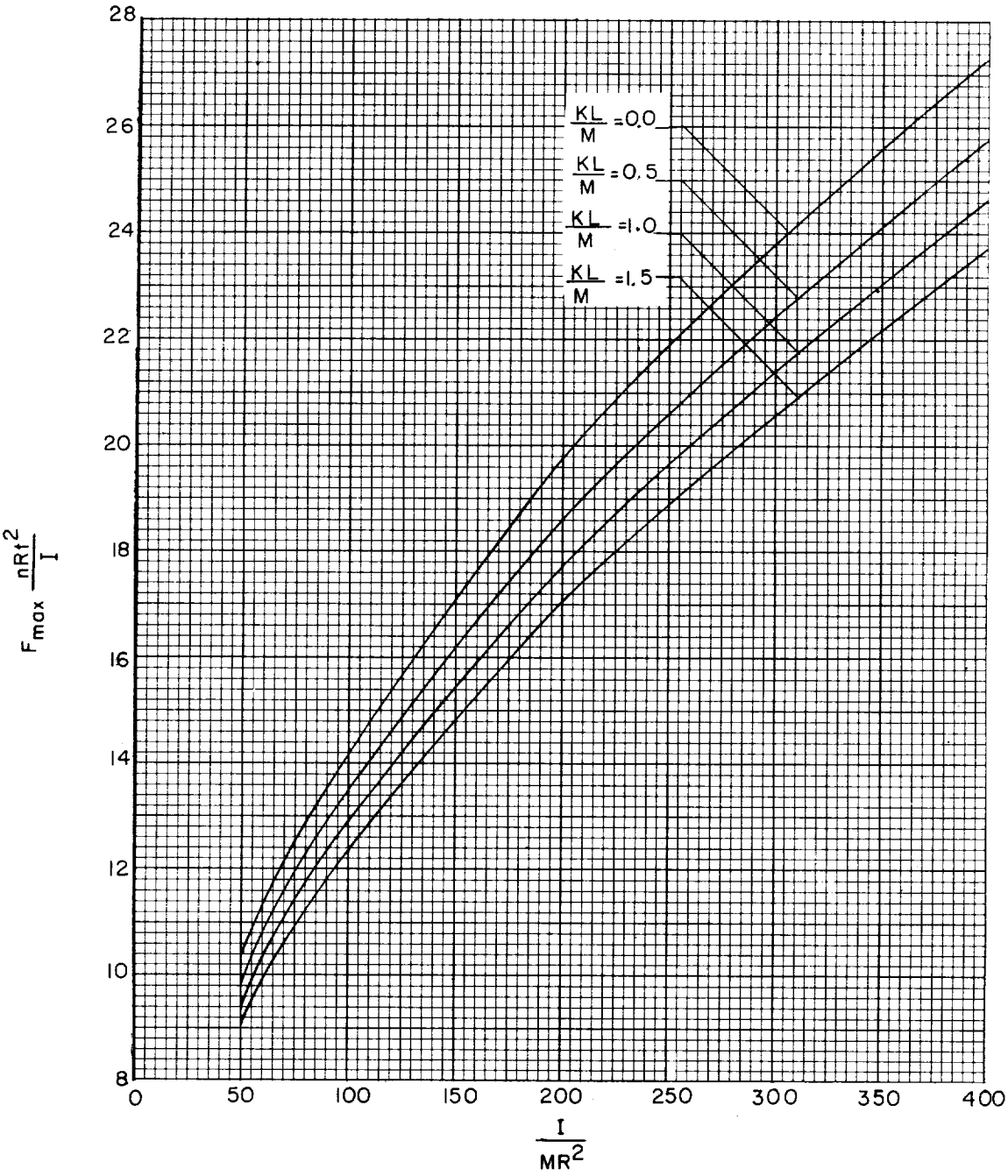

(a) $\lambda = 0.00$.

Figure 15.- Variation of $F_{max} \frac{nRt^2}{I}$ with $\frac{I}{MR^2}$ for various values of $\frac{KL}{M}$ and λ.

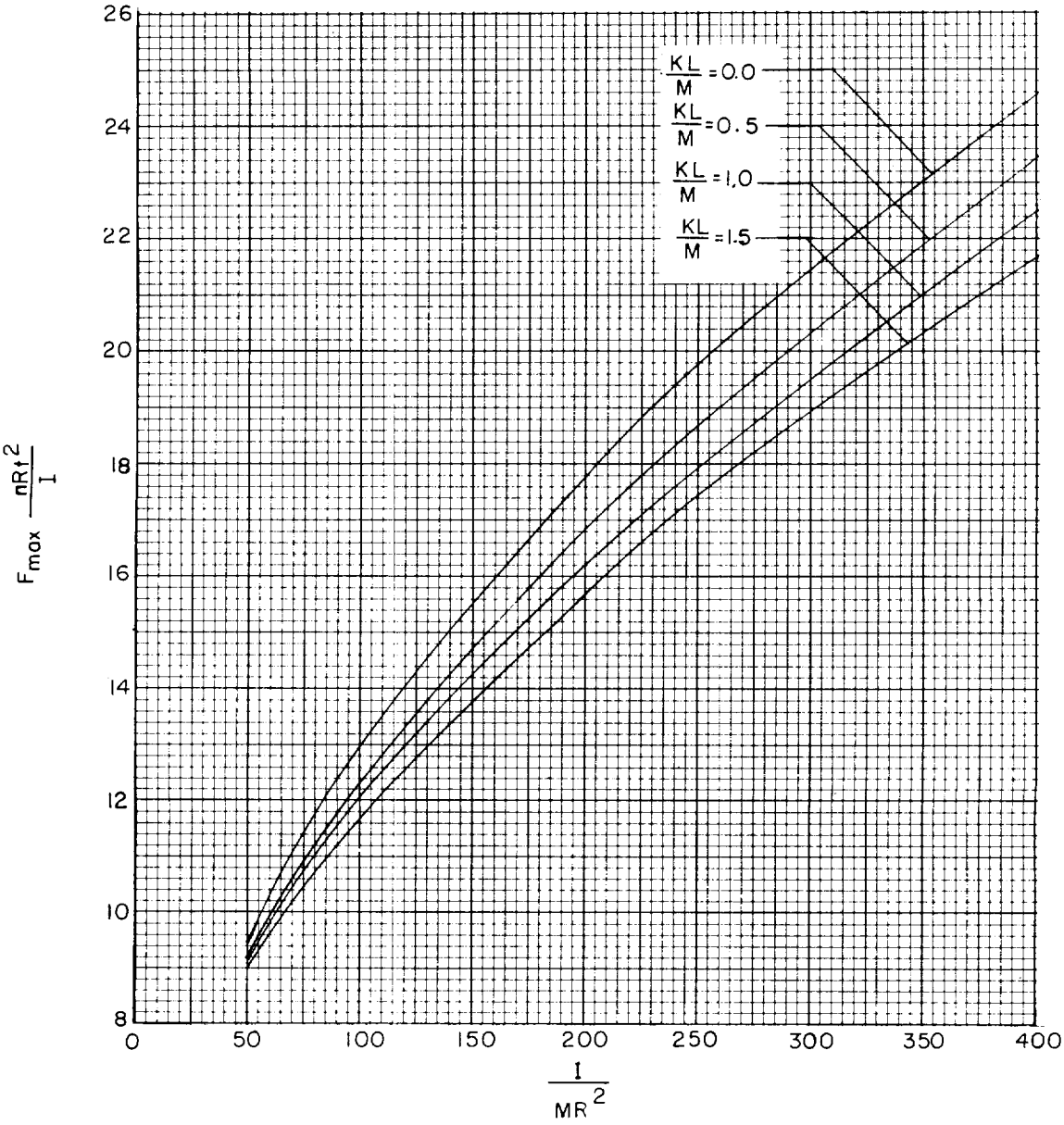

(b) $\lambda = 0.05$.

Figure 15.- Continued.

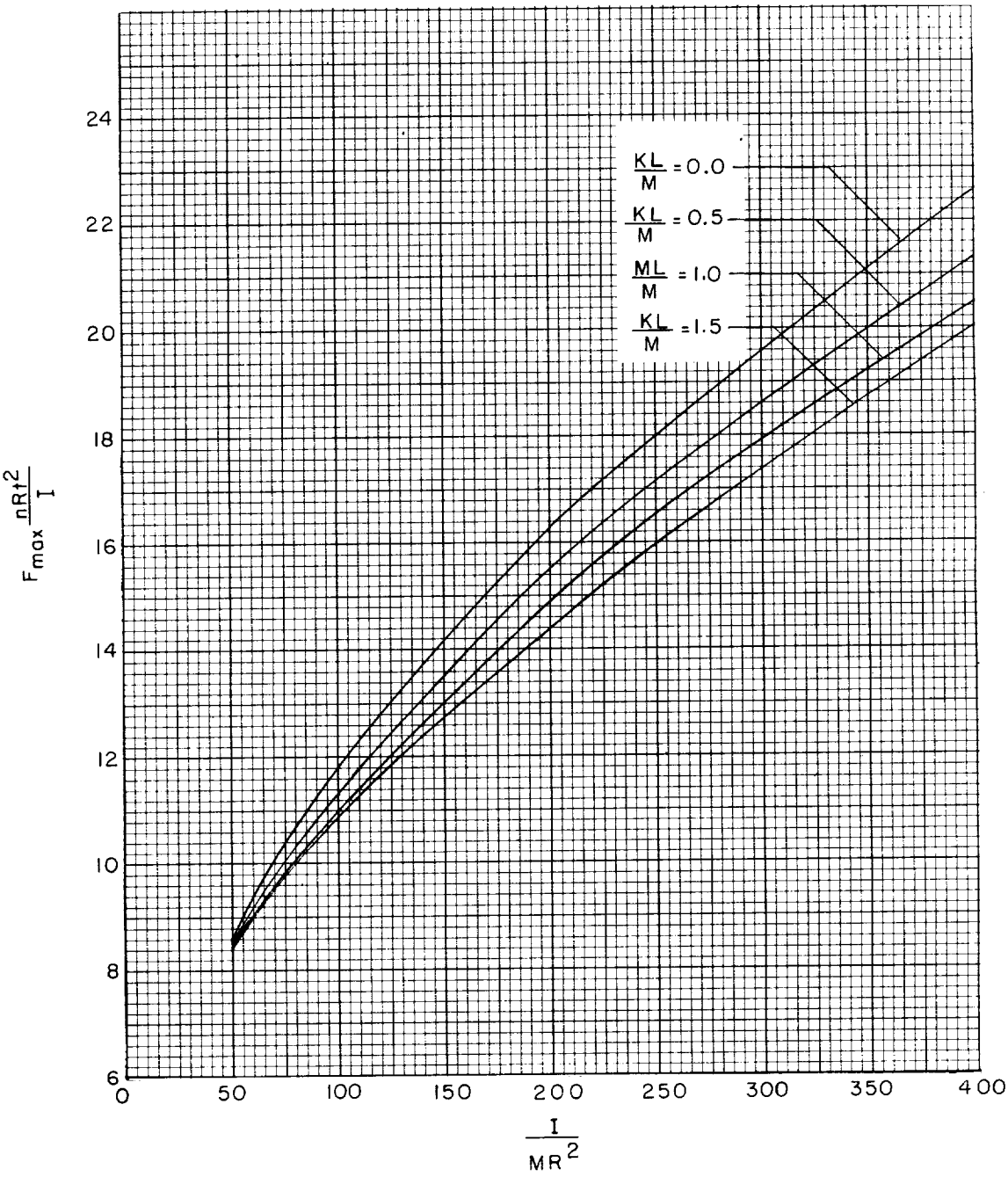

(c) $\lambda = 0.10$.

Figure 15.- Continued.

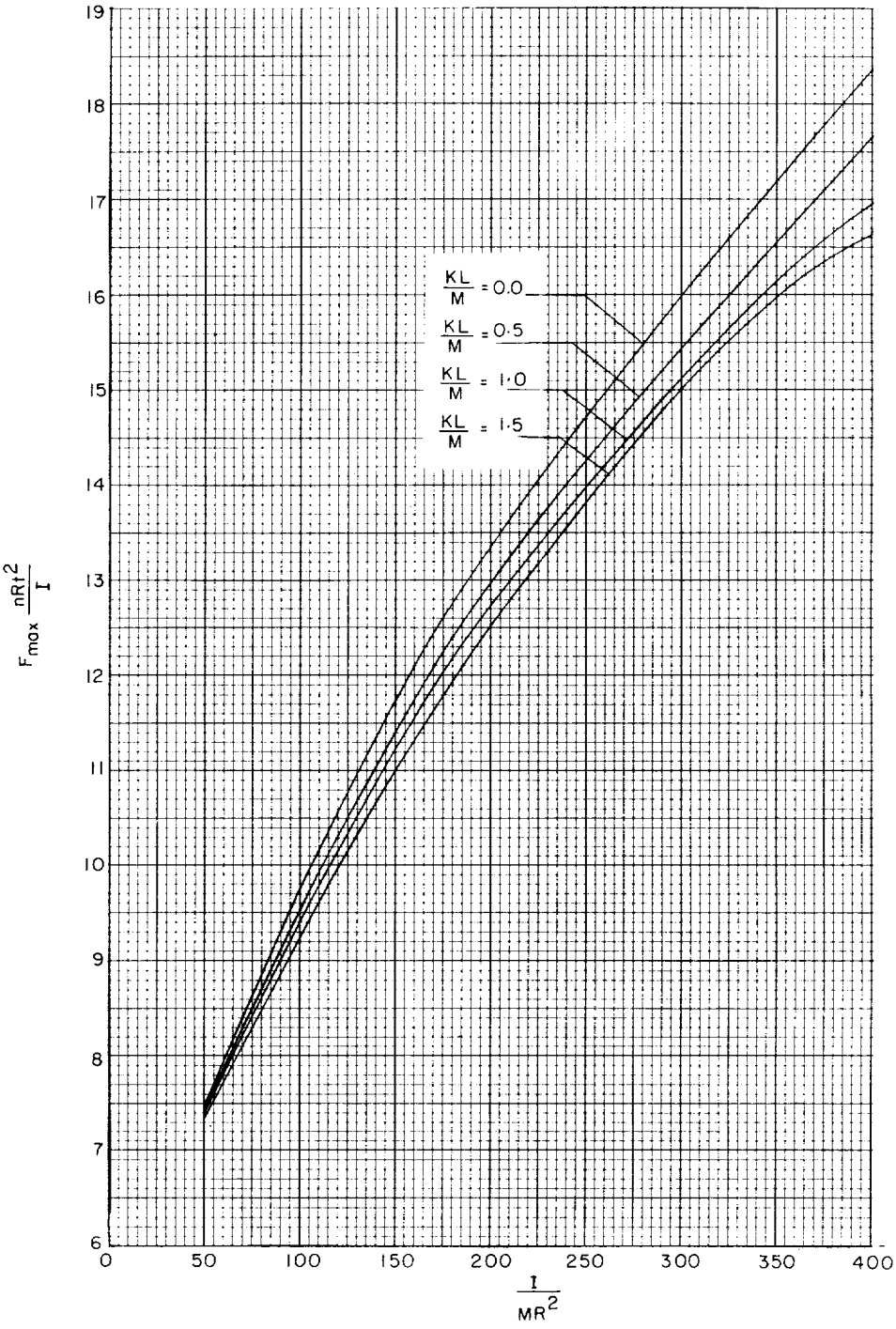

(d) $\lambda = 0.20$.

Figure 15.- Concluded.